

# LINEAR TECHNOLOGY

MAY 1995

VOLUME V NUMBER 2

## ***IN THIS ISSUE . . .***

### **COVER ARTICLE**

**Big Power for Big Processors: The LTC<sup>®</sup>1430 Synchronous Regulator... 1**

Dave Dwelley

**Editor's Page ..... 2**

Richard Markell

**LTC in the News ..... 2**

### **DESIGN FEATURES**

**Power Factor Correction, Part Two — Filling in the Boxes ..... 3**

Dale Eagar

**The LT<sup>®</sup>1319: A Light-to-Digital Converter for Infrared Communications ..... 7**

George Feliz

**The LTC1392: Temperature and Voltage Measurement in a Single Chip ..... 10**

Ricky Chow and Dave Dwelley

**LT1580 Low-Dropout Regulator Uses New Approach to Achieve High Performance ..... 13**

Craig Varga

**Quad Current-to-Voltage Converter is Ideal for Optical Disk Drives ..... 15**

William H. Gross

**Design Ideas ..... 22-37**  
(complete list on page 22)

**New Device Cameos ..... 38**

**Design Tools ..... 40**

**Sales Offices ..... 40**

## **Big Power for Big Processors: The LTC1430 Synchronous Regulator**

by Dave Dwelley

### **Introduction**

As computer technology advances, microprocessor designers pack more and more transistors into less and less space with each new design. In an effort to save power and reduce heat, many of the newest microprocessors run from nonstandard supply voltages well below the traditional 5V, often with supply tolerance requirements tighter than the typical  $\pm 5\%$ . Those millions of transistors, all switching at the same time, require prodigious amounts of current from the low-voltage supply. Additionally, many of the supporting chips still require 5V supplies; this forces system designers to generate multiple high-power, nonstandard output voltages. Last minute power-supply voltage changes by microprocessor manufacturers and differing voltage requirements for otherwise pin-compatible processors add to the confusion and risk in such designs. A popular solution is to add a secondary DC/DC converter on the motherboard to convert the 5V main supply to the lower supply the microprocessor requires. For this purpose, Linear Technology introduces the LTC1430 high-power switching-regulator controller, targeted specifically at high-power, 5V step-down applications where efficiency, output-voltage accuracy, and board-space requirements are critical.

### **Functional Description**

The LTC1430 is a new switching-regulator controller designed to be configured as a synchronous buck converter with a minimum of external components. It runs at a fixed switching frequency (nominally 200kHz) and provides all timing and control functions, adjustable current limit and soft start, and level-shifted output drivers designed to drive an all-N-channel synchronous buck converter architecture. The switch driver outputs are capable of driving multiple, paralleled power MOSFETs with submicrosecond slew rates, providing high efficiency at very high current levels while eliminating the need for a heat sink in most designs. The LTC1430 is usable in converter designs providing from a few amps to over 50A of output current, allowing it to supply 3.3V power to the most current-hungry arrays of microprocessors. A novel "safety belt" feedback loop provides excellent large-signal transient response with the simplicity of a voltage-feedback design. The LTC1430 also includes a micropower shutdown mode that drops the quiescent current to 1 $\mu$ A.

The LTC1430 is designed to be used in an all-N-channel synchronous buck architecture (Figure 1, page 19), allowing the use of cost-effective, high-power N-channel

*continued on page 19*



**LT**, LTC and LT are registered trademarks of Linear Technology Corporation. Burst Mode is a trademark of Linear Technology Corporation. Pentium is a trademark of Intel Corporation. PSpice is a trademark of MicroSim Corporation.

# Hot Products for Hot Processors

by Richard Markell

How many of us in today's so-called information age have lost information or had a computer system crash? Might this have been a result of poor power-supply design and implementation? It's really hard to say how many system crashes are the result of power supplies that cannot output the required current, stay within the voltage tolerances, or provide the transient response demanded. What is certain is that the situation will get worse. Future Pentium™ and P6 processors and processors from other vendors hoping to plug into these sockets will undoubtedly demand stricter power-management solutions than are currently required.

Linear Technology leads the industry in supplying devices and circuits to provide reliable, cost-effective solutions for powering all types of computer systems, from desktop systems to small, handheld devices. This issue provides insight into several new devices from LTC for powering the next generation of computer products.

This issue's lead article highlights the LTC1430 synchronous switching-regulator controller. The LTC1430 is specifically designed to provide high currents at the precise voltages required by today's and tomorrow's microprocessors. The LTC1430 converts the 5V main supply (in the silver box) to the lower supply voltage required by the microprocessor. It does all this with efficiencies approaching 95% and the excellent transient response required to meet the specifications set by most microprocessor vendors. This issue also introduces the LTC1392, a single-chip data-acquisition system for temperature, voltage, and current measurement. The LTC1392 can be used as an environmental monitor inside a computer. No external components are required for temperature or voltage measurements; current measurements can be configured with a single resistor.

The device provides a 10-bit digital output through a three- or four-wire serial interface that can talk to virtually any microprocessor.

The LT1580 is a new, very low-dropout NPN regulator for powering desktop microprocessor-based computers and systems. The LT1580 can supply all but the most extreme of the many voltages that today's microprocessors require and that tomorrow's will demand. The LT1580 requires a supply voltage higher than the main power source (for example, 12V) to provide the power for the control circuitry and to provide the drive for the NPN output stage. The LT1580 has excellent transient response, and can provide currents up to 7A with a 0.8V input-to-output voltage differential. The LT1311 is a quad current-to-voltage converter useful for photon-to-electron conversion and other I-to-V applications. The LT1311 design is based on a new approach to I-to-V conversion, which provides superior DC and AC performance without external DC trims or AC frequency compensation. The -3dB bandwidth of the LT1311 is 12MHz and its settling time is less than 175ns to 0.1% for a 2V output step. The LT1311 is ideal for converting multiple photodiode currents to voltages and for general-purpose matched inverting amplifier applications.

The LT1319 is LTC's dedicated light-to-digital converter IC. The LT1319 is a flexible, general-purpose building block that contains all the circuitry necessary to convert modulated photodiode current into a digital signal. The LT1319 is flexible enough to be configured for a variety of standards, including IrDA-SIR, Sharp/Newton, FIR, and 4PPM. This issue also features the second part of the Power Factor Correction article begun in the last issue.

Finally, we present many useful design ideas, circuits that provide proven, tested designs for specific applications. ⚡

## LTC in the News...

In the April 13, 1995 issue of *EDN Magazine*, the results of voting by EDN's readership showed none other than Bob Dobkin, LTC's V.P. of Engineering, as EDN's "Innovator of the Year." This is the fifth year for EDN to have their readership nominate and vote for the Innovation and Innovator of the Year. Congratulations to Bob and thanks to all of you who voted for him.

LTC posted a new record for net sales at \$68,135,000 for the quarter ended April 2, 1995, an increase of 32% over the third quarter of the previous year. Net income for the quarter also hit a new high at \$21,805,000 representing an increase of 43% over the third quarter of last year. In addition, the Company paid a cash dividend of \$0.07 on May 17, to shareholders of record on April 28, 1995.

*Financial World*, April 1995, named LTC in its "Independent Appraisals" section showing the top 900 over-the-counter traded companies in terms of market capitalization. Within this list, LTC received an A+ (superior) rating based on five criteria emphasizing recent growth and profitability.

In the April 1995 edition of *Electronic Business Buyer* magazine, our President and C.E.O., Robert Swanson is interviewed by Bob Ristelhueber in the "Market Pulse" section which focuses on trends in the analog market. In it, Mr. Swanson points out that despite dire predictions for the future of analog, the need for high performance analog has continued to grow. As Mr. Swanson put it, "...no digital solution has eliminated the need to interface to the analog world, ....they've just created new opportunities for analog..." ⚡

# Power Factor Correction, Part Two — Filling in the Boxes

by Dale Eagar

In part one of this article, we investigated power factor correction (PFC) by looking at its line frequency voltage, current, and power waveforms. The device that performs PFC is called a power factor correction conditioner (PFCC).

The waveforms shown in part one are ideal, in that they reflect an average of what is happening inside the three boxes, ignoring higher frequency effects. We showed that PFC could be performed if the appropriate components were implemented. We further developed the concept of an instantaneously adjustable DC variac as an equivalent circuit for the power handling part of the PFCC. In part two, we will develop the circuitry for the implementation of the DC variac by introducing the boost converter.

## Why the Boost Converter?

Even though several circuit configurations can perform PFC conditioning, the boost topology is by far the most popular, because of the topology's inherently low input ripple current. This ripple current is at the switching frequency of the boost converter, and must be filtered by an EMI filter at the input terminals of the PFCC. Unfiltered switching-frequency ripple may be conducted down the power line as EMI.

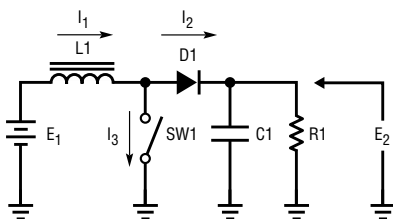


Figure 1. Simple boost converter

## An Ideal Boost Converter

A simple boost converter is shown in Figure 1. The boost converter has two modes of operation, each with its own characteristics. The two modes are known as *discontinuous mode* and *continuous mode*. A boost converter functioning as a PFCC will operate in both modes. The criterion for determining in which of these two modes a switcher is running at any given time is whether the inductor is left unloaded for any part of a switching cycle (transitions don't count). If the inductor is unloaded (SW1 and D1 both off) during a switch cycle, the switcher is operating in the discontinuous mode. With the circuit shown in Figure 1, operation becomes discontinuous when the inductor current decays to zero. This happens during the part of the switching cycle when SW1 is open.

To understand the workings of a switching regulator, it is necessary to have at least a mild immunity to "inductorphobia."

*The global outbreak of Inductorphobia of the late 20th century threatened to wipe out all analog circuit design. Fortunately, the requirement for power factor correction mandated the use of the inductor. This use is largely responsible for the continuation of the practice of the art through the black age of digital design. [See "The Black Age." History of the Sol System, Volume 17, p. 12,947]*

Immunization against Inductorphobia involves exposing oneself to inductors, and is highly recommended.

When used in a boost-mode converter, the inductor is placed across the input line and allowed to intercept and store some energy. The inductor is then placed between the input and the output to dump its energy, (along with some additional intercepted line power) into the load.

## An Introduction to the Ideal Inductor

1. An ideal inductor will act to prevent DC voltage across its terminals. The inductor will steal energy from any source that attempts to impose a voltage across its terminals.
2. An ideal inductor will store the minimum possible energy. The inductor will attempt to dump any energy that it has stolen at the first possible moment.
3. An ideal inductor, having an inductance of L, will stretch and store L volt seconds of charge for each ampere of current flowing through it. The inductor will relax and return L volt seconds of charge to the circuit upon withdrawal of each ampere of current flow.

If, during a switch cycle, the inductor can successfully unload all of its energy, the operating mode is said to be discontinuous. Otherwise, the inductor is forced to store some amount of energy through multiple switch cycles. The presence of such stored energy indicates the continuous mode of operation.

When used to implement a DC variac, a boost-mode switcher controls the duty cycle of the switch SW1 so that the volt seconds across the inductor always add up to zero over any complete switching cycle.

## The Continuous-Mode Boost Converter

In the steady state, the continuous-mode boost converter implements the function of the DC variac. The duty factor is set by the constraint on volt seconds, namely that the total volt

seconds imposed on the inductor will be zero when looked at over a complete switch cycle.

The voltage transformation ratio of the DC variac is:

$$E_2/E_1 = 1 + DF/(1 - DF)$$

where DF = Duty Factor

Some interesting properties of this DC variac are:

- DF = 0,  $E_2 = E_1$
- DF = 0.5,  $E_2 = 2 \times E_1$
- DF = 1,  $E_2 = \text{Infinity}$

It's easy to see that as duty factor approaches unity, things get interesting, and can, in fact, become quite a problem.

The problem is not merely that you get infinite voltage, but that you get infinite voltage and infinite current at the same instant—that means infinite power, which tends to rearrange galaxies.

We know that this is a problem, because after a past catastrophic galactic self destruction, we sent scout ships to the estimated center of the galaxy, only to find a breadboard of the circuit shown in Figure 1 floating in space with switch SW1 open. Evidently, ideal components don't vaporize.

One interesting property of a boost converter with a DF of unity is that the switch SW1 never opens, which can be good or bad. In the non-ideal boost converter, the switch simply blows up, limiting current. In the ideal circuit, the power stored in L1 increases with the square of the du-

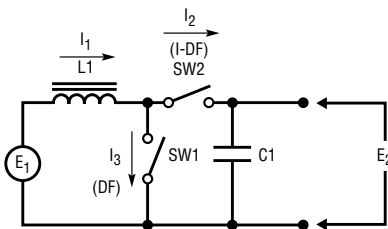


Figure 2a. Continuous-mode boost converter

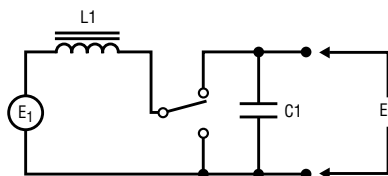


Figure 2b. Simpler version of Figure 2a

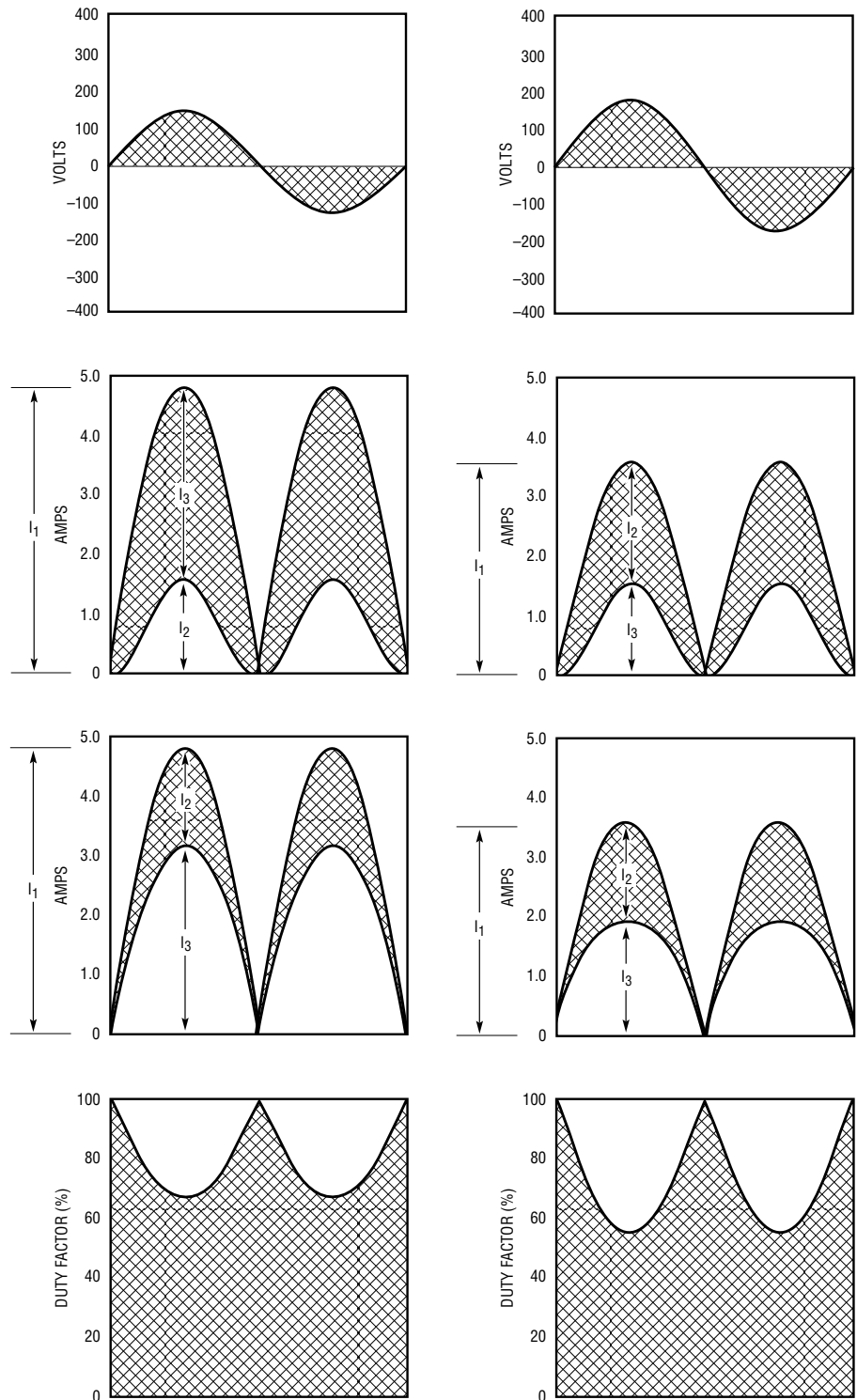


Figure 3. Waveform gallery

ration of the time SW1 is closed. This leads us to one final statement about the boost converter with a unity DF:

If, in your engineering adventures you happen across the circuit shown in Figure 1, implemented with ideal

components, and with the switch SW1 closed, do not open SW1! Call 911, and, for added safety, take the first hyper-light shuttle out of the galaxy!

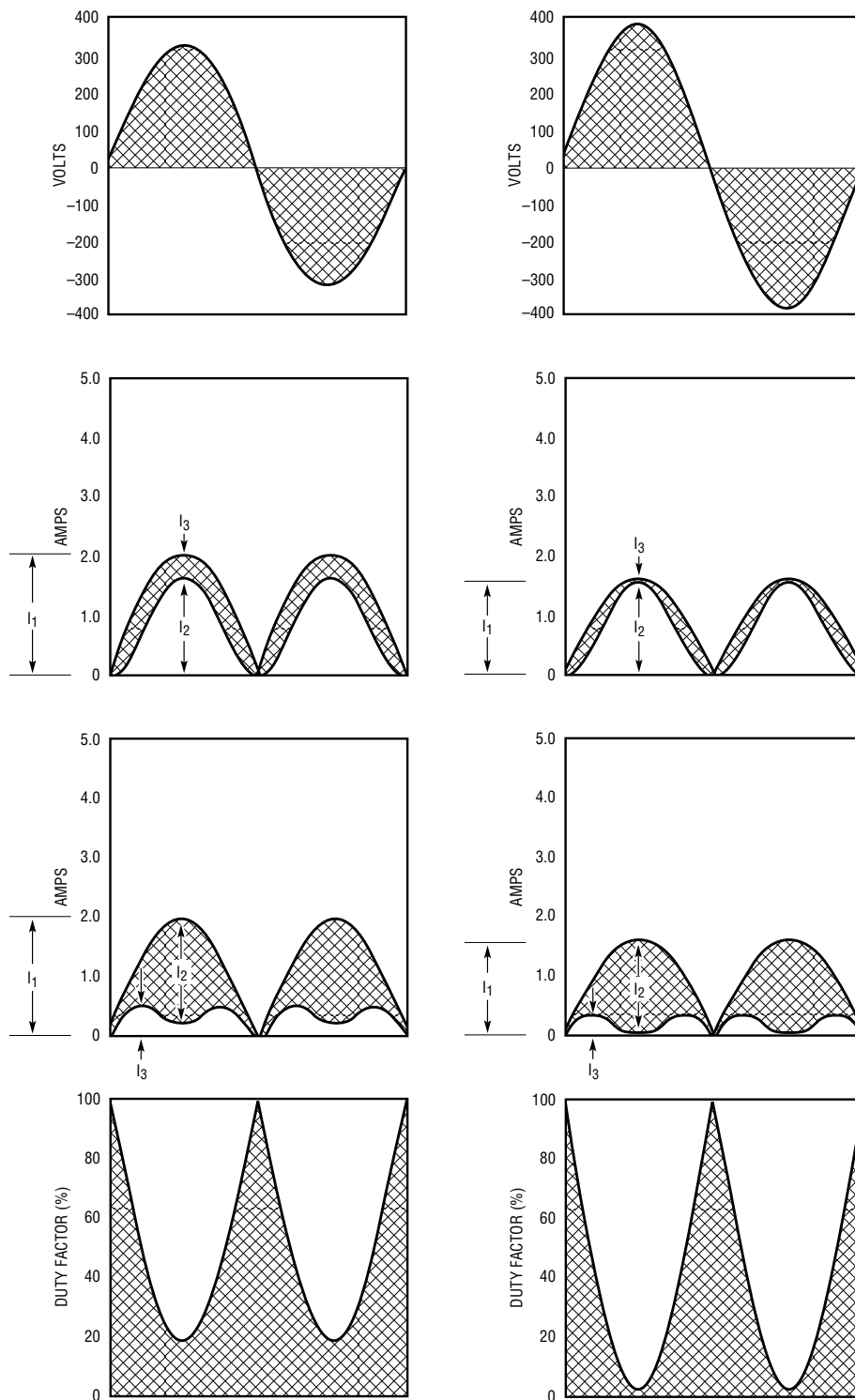


Figure 3. Waveform gallery (continued)

values of  $I_1$ ,  $I_2$ , and  $I_3$ . Thus, Kirchhoff's laws apply to the averaged steady-state values of  $I_1$ ,  $I_2$ , and  $I_3$  just as it applies to the instantaneous values. Once past all of that linear system stuff, we can get to much more interesting things like circuits and waveforms.

To implement a continuous-mode PFCC with a boost converter, a slight modification needs to be made to the circuit in Figure 1. The modification involves the substitution of a second switch SW2 for the output diode D1, as shown in Figure 2a. The opening and closing of the switch SW2 is out of phase with the opening and closing of SW1. Thus, the action of SW1 and SW2 constitutes a single-pole, double-throw switch, as shown in Figure 2b. This modification causes the boost converter to *always* operate in the continuous mode.

Figure 2b details this continuous-mode boost converter implementation of the PFCC. Figure 3 shows the waveforms of the PFCC shown in Figure 2b. One can see that the duty factor is changing continuously, and is directly related to the input voltage. An interesting property of the continuous-mode boost converter is that the duty factor does not change significantly with load current. (This is to be expected for a collection of things whose purpose is imitating a DC variac.)

The circuit of Figure 2b is not trivial to implement in the real world. It not only requires a switch to be substituted for D1 (Figure 1), but also requires four additional switches to implement the input rectifier bridge (so conveniently missing from Figure 2b).

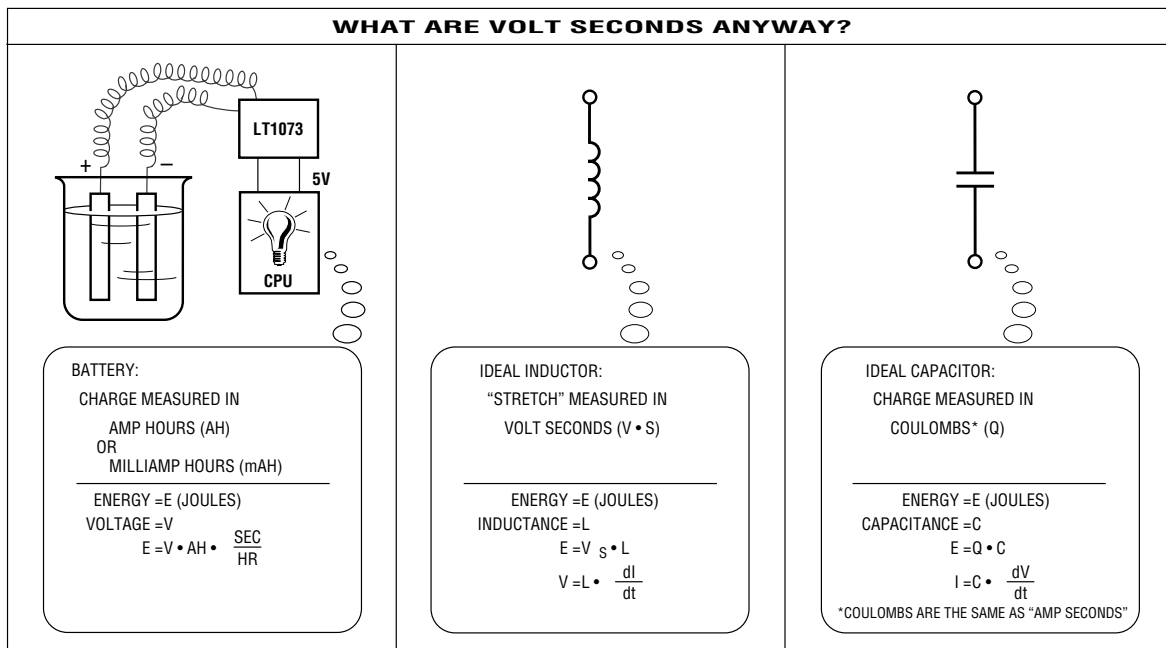
### The Nonsteady-State Boost Converter Operating in Continuous Mode

One of the problems of an ideal approach to a problem like PFC is oversimplification. Here we have developed a model for a DC variac that works wonderfully well in all steady-state conditions. If the load current changes, does the duty factor need to change?

### The Continuous Boost Converter as a PFCC

By setting the switching frequency of the boost converter to many hundreds to several thousand times the line frequency, we get the freedom to analyze the boost converter in terms

of average values over multiple cycles. Because the system detailed in Figure 1 behaves as a linear system in both states of SW1, the average values of  $I_1$ ,  $I_2$ , and  $I_3$  will obey the same laws obeyed by the instantaneous



The answer is both yes and no. The model of the DC variac is not quite accurate for a continuous-mode boost converter. The real model of the DC variac needs to include inductance L1 in series with the input. The net effect of L1 in the model of the DC variac can be seen when the system responds to steps in current at fixed input and output voltages. To allow a change in current, L1 will capture and store L1 volt seconds per amp of current change. The duty factor will have to change momentarily from the steady-state value to allow the choke to capture the needed volt seconds. This is illustrated in Figure 4.

In the working PFCC, the effect of

capturing and releasing volt seconds is seen in a slight shift in phase of the duty factor waveform. The amount of phase shift is determined by the value of L1, and is negligible for all practical purposes.

**Conclusion**

The boost converter can be used to implement the DC variac function required to perform PFC, but this requires the duty factor to be well controlled.

In part three of this series, we will investigate the discontinuous-mode boost converter and how it differs from the continuous-mode boost converter. **LT**

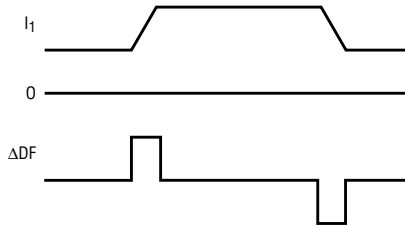


Figure 4. Current in the ideal choke and duty factor

**Volt Seconds** — the measure of the area under the curve of voltage when plotted against time in the Cartesian coordinate plane. The volt second, the unit of measure of stretch, was popularized in the late 20th century with the advent of the switching power supply. Later in the 21st century, the volt second took on its present sinister meaning when Sumlioux Midge was sentenced to twelve million volt seconds for making the absurd statement “Digital electronics is a mere subset of analog electronics.” Midge made the now infamous statement in 2027 near the peak of the “Era of Digital Decadence.” [Solclopedia, 2120. Volume V, p. 324.]

**Stretch** — The measure of lattice deformation due to magnetostriction in a ferromagnetic material. Stretch is also used to describe the presence of volt seconds in an inductor. This usage is not strictly canonical in that it is used irrespective of the medium that actually contains the magnetic lines of force. —Solclopedia, 2120 Volume V, p. 285.

# The LT1319: A Light-to-Digital Converter for Infrared Communications

by George Feliz

Infrared communication will soon provide a convenient, cableless, point-to-point connection between portable computers, PDAs (personal digital assistants), desktop computers, and peripherals. Several communication standards exist, including IrDA-SIR (Infrared Development Association-Serial Infrared) and Sharp/Newton ASK (amplitude-shift keying), and more standards are being developed. The LT1319 is a flexible, general-purpose building block that contains all the circuitry necessary to transform modulated photodiode current to a digital signal. When coupled to an external photodiode, the LT1319 becomes a light-to-digital converter that can be configured to receive multiple standards. The LT1319's flexibility is a key feature because of the vast differences between standards and because it can be reconfigured for future standards.

## Operation of the LT1319

Figure 1 is a block diagram of the LT1319 with external filters for IrDA-SIR and Sharp/Newton. The preamp is the secret of the part's versatility. An external photodiode connected to the preamp input produces a reverse current proportional to the incident light. The preamp is a low-noise ( $2\text{pA}/\sqrt{\text{Hz}}$ ), high-bandwidth (7MHz) current-to-voltage converter that transforms the photodiode current ( $I_{\text{PD}}$ ) into a voltage. The 7MHz bandwidth supports data rates up to 4Mbaud. The low noise allows for links of two meters or more. When full bandwidth is not required, sensitivity can be increased by further reducing the noise with a lowpass filter on the preamp output. Encircling the preamp

is a loop formed by  $\text{GM1}$ ,  $\text{C}_{\text{F1}}$ , a buffer, and  $\text{R}_{\text{L1}}$ . For low-frequency signals, the loop forces the output of the preamp to  $V_{\text{BIAS}}$ . High-frequency signals are unaffected by the loop, so the preamp output is effectively AC coupled. The break frequency set by  $g_{\text{m}}$ ,  $\text{C}_{\text{F1}}$  and the ratio of  $\text{R}_{\text{FB}}$  to  $\text{R}_{\text{L1}}$  is easily modified, since  $\text{C}_{\text{F1}}$  is a single capacitor to ground. The loop rejects unwanted ambient signals, including sunlight and incandescent and fluorescent lights.

After the preamp stage, there are two separate channels, each containing a high-input-impedance filter buffer, two gain stages with lowpass loops, and a comparator. The only difference between the channels is the response times of the comparators—25ns and 60ns, respectively. For modulation schemes with pulse widths down to 125ns, the high-frequency comparator with its active pull-up output stage is ideal. The low frequency comparator, with its open-collector output and 5k internal pull-up resistor, is suitable for more modest speeds, such as the 1.6 $\mu\text{s}$  pulses seen with IrDA-SIR. Buffers A1 and A4 allow the use of a wide range of external filtering to optimize sensitivity and selectivity for specific modulation methods. The external components shown are an 800kHz lowpass for IrDA-SIR, formed by  $\text{R}_{\text{F2}}$  and  $\text{C}_{\text{F3}}$ , and a 500kHz LC tank circuit with a Q of 3 for Sharp/Newton, formed by  $\text{R}_{\text{F1}}$ ,  $\text{C}_{\text{F2}}$  and  $\text{L}_{\text{F1}}$ . The loops containing GM2 and GM3 surround the gain stages and function similarly to the preamp loop. They also provide accurate threshold setting at the comparator inputs by forcing the DC level of the differential gain stages to zero.

The threshold is set by the current into pin 11, which is multiplied by 4 in the  $V_{\text{TH}}$  generator and then sunk through  $\text{R}_{\text{C1}}$  and  $\text{R}_{\text{C3}}$ . With an  $\text{R}_{\text{T1}}$  of 30k, the current into pin 11 is about 130 $\mu\text{A}$ . The comparator thresholds are  $130\mu\text{A} \times 4 \times 500\Omega = 260\text{mV}$ . Referred to the filter buffer inputs, the threshold is  $260\text{mV}/400$  or 0.65mV.

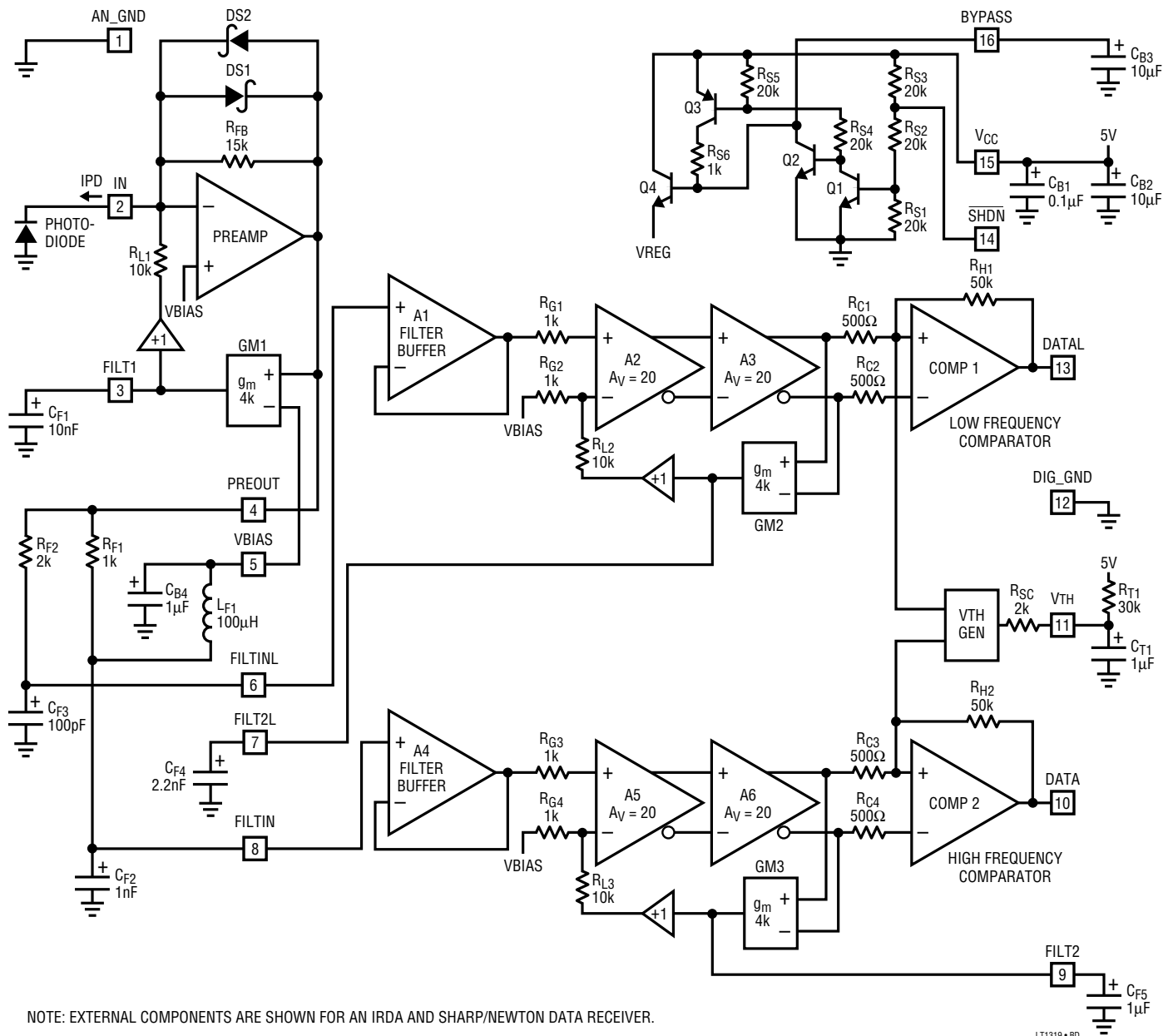
Other features of the LT1319 include a shutdown pin, which reduces the supply current from a nominal 14mA to 500 $\mu\text{A}$ . To reduce false output transitions due to power-supply noise, the preamp and gain stages have separate analog grounds and are operated off an internally regulated 4V supply bypassed at pin 16. The comparators, shutdown, and threshold circuitry operate directly off the 5V supply and are returned to digital ground. To provide a low-noise bias point for the amplifiers, the part generates an internal 1.9V reference ( $V_{\text{BIAS}}$ ), which is bypassed externally at pin 5.

## Filtering

Optimal filtering rejects interference and improves sensitivity. Although the LT1319 data sheet shows filtering for several modulation standards, there are applications that require custom filtering. Here are some filter guidelines:

1. Limit the noise bandwidth with a lowpass filter that has a rise time equal to half the pulse width. For example, for 1 $\mu\text{s}$  pulses, a 700kHz lowpass filter has a 10%–90% rise time of 500ns.

2. Limit the maximum highpass break frequency to  $1/(4 \times \text{pulse width})$ . For 1 $\mu\text{s}$  pulses, the limit would be 250kHz.



NOTE: EXTERNAL COMPONENTS ARE SHOWN FOR AN IRDA AND SHARP/NEWTON DATA RECEIVER.

LT1319 • 8D

Figure 1. LT1319 block diagram

3. In setting the highpass filters, space the filter corners by a factor of 5–10 to reduce overshoot due to filter interaction. Overshoot becomes especially important for high input levels, because it can cause false pulses that may not be tolerated in certain modulation schemes.

4. As a general rule, place the lowest frequency highpass around the preamp and the highest highpass around the gain-of-400 stage, or between the preamp and the filter-buffer inputs. The reason for this order is that high light levels can have slow photodiode-current tails that can increase the output pulse width. The

tail response can be filtered out by a highpass of 200kHz–400kHz.

5. In all cases with custom filtering, or when modifying one of the applications presented in the data sheet, evaluate the system at a variety of distances and with data streams that exhibit the full duty-cycle range.

### Overdrive at Short Range

At short range there are two major problems: huge photodiode currents and slow photodiode-current decay. Typically, the maximum photodiode current that the LT1319 can handle is 6mA. Beyond this level the preamp input voltage can sag and its recovery time can cause wide pulse widths at the output. The maximum input current can be increased to 20mA or more by placing an NPN transistor with its emitter tied to pin 2, its base tied to pin 4, and its collector tied to the 5V supply. The choice of transistor depends on the bandwidth required for the preamp. The base-emitter capacitance of the transistor ( $C_{JE}$ ) is in parallel with the 15k feedback resistor of the preamplifier and performs a lowpass filtering function. For modest data rates, such as IrDA-SIR and Sharp/Newton, a 2N3904 limits the bandwidth to 2MHz, which is ample. For data rates with pulses narrower than 500ns, a transistor

with  $f_T$  greater than 1GHz is needed, such as MMBR941LT1.

The second problem with large input signals is the photocurrent tail. This tail is proportional to the input level and has a decay time constant greater than 1 $\mu$ s. If the data has a low duty cycle and the highpass filtering is below 200kHz, the output pulse width can become so wide that it extends into the next bit interval. For the case of IrDA-SIR, rejecting the 1 $\mu$ s time constant can cause attenuation of the data pulses and reduced maximum-link distance. An alternative is shown in Figure 2: an application for IrDA-SIR and two of its proposed higher-data-rate extensions—FIR and 4PPM. A clamp/squelch circuit consisting of Q1, Q2, and RC1-RC4 is added. Q1 is used as described above to clamp the input, but the input-current level at which the clamp engages has been modified by RC1 and RC2. Without the resis-

tors, Q1 would turn on when the voltage across the 15k resistor in the preamp reached about 0.7V (an input of 47 $\mu$ A). The drop across RC1 reduces this voltage by about 350mV. At this new level of 23 $\mu$ A, Q1 turns on to clamp the preamp output. The collector current of Q1 provides base drive for Q2, which saturates and pulls its collector close to 5V. The FILT2 and FILT2L inputs are now pulled positive by RC3 and RC4, which force an offset at the inputs to the filter buffers that is high enough to reject the input tail.

### Conclusion

The LT1319 is an ideal choice for an infrared receiver because its high performance and flexibility allow it to implement multiple modulation schemes. Point-to-point infrared links built around the LT1319 conform to today's standards and are easily modified for the standards of tomorrow. 

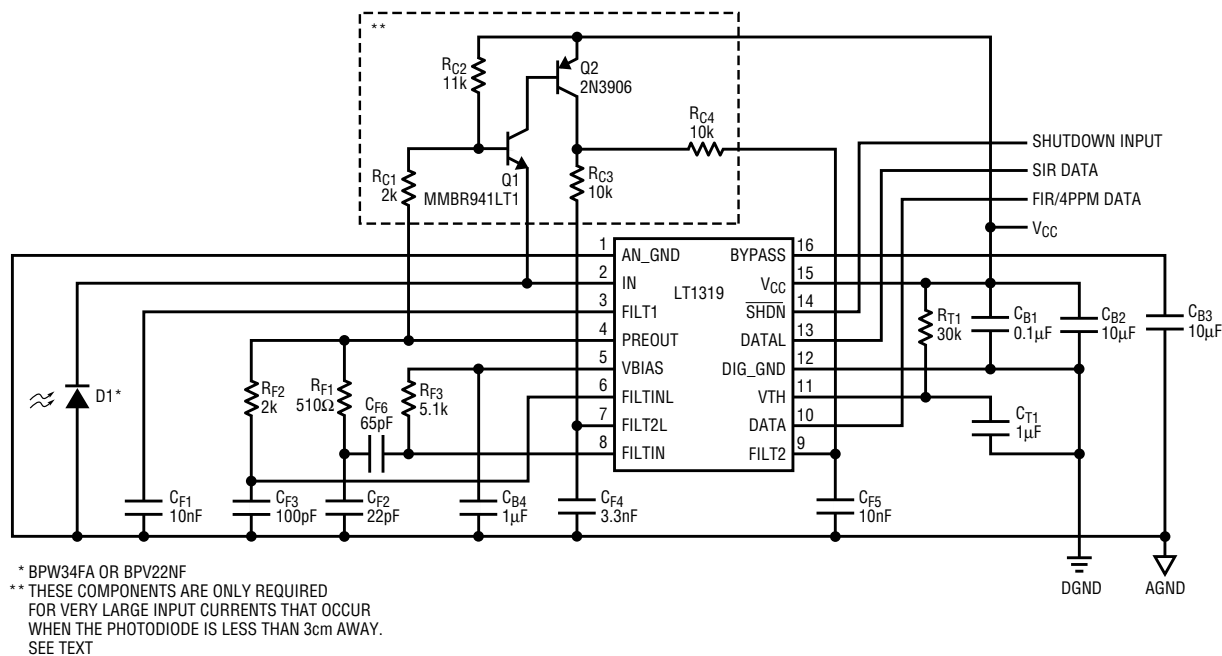
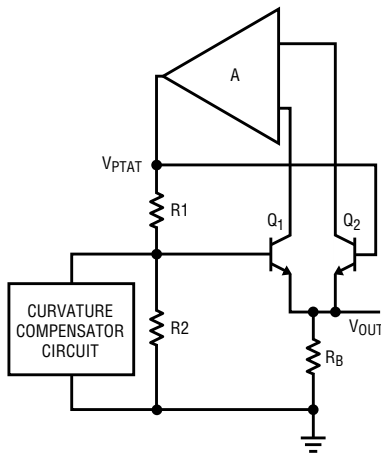


Figure 2. IrDA SIR/FIR/4PPM data receiver





**Figure 2. Block diagram of Celsius temperature sensor**

and the thermal mass of the package, keeps the die temperature to within  $0.1^\circ$  of ambient temperature for single conversions; continuous temperature conversions with no idle periods in between will raise the die temperature no more than  $0.25^\circ$  above ambient temperature. The temperature-sensor cell is based on a circuit devised in 1979 by G. C. M. Meijer of the Delft University of Technology, The Netherlands. The circuit generates a current proportional to absolute temperature ( $I_{PTAT}$ ), and subtracts from it a current proportional to the  $V_F$  of a P-N diode. Meijer showed that the resulting current is inherently calibrated when it is properly trimmed at any one temperature. The LTC1392 temperature sensor (Figure 2) takes advantage of this basic principle to generate a voltage proportional to temperature by generating a  $V_{PTAT}$  voltage and subtracting  $V_F$  directly from it. Referring to Figure 3a, it can be shown that the total output voltage is scaled proportionally to the Celsius temperature of the system. The circuit includes a curvature-compensation circuit to compensate for the inherent non-linearity of  $V_F$  versus temperature (Figure 3b).

**Measurement Performance**

Wafer-level trimming allows the LTC1392 to achieve a guaranteed accuracy of  $\pm 2^\circ\text{C}$  at room temperature, and  $\pm 4^\circ\text{C}$  over the entire

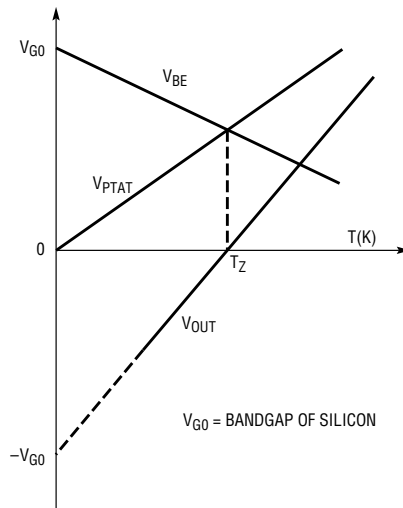


**Figure 3a. Idealized output voltage,  $V_{OUT}$ , and its components versus temperature**

operating temperature range. The 10-bit A/D gives  $0.25^\circ$  resolution over the  $0^\circ\text{C} - 70^\circ\text{C}$  (LTC1392C) or  $-40^\circ\text{C} - 85^\circ\text{C}$  range. To calculate temperature from the LTC1392's output, use the formula  $(\text{ADC code}/4) - 130^\circ$ . The theoretical maximum range is  $-130^\circ$  to  $125.75^\circ$ , although the LTC1392 isn't guaranteed to meet spec over this whole range. Figure 4 shows the typical output temperature error of the LTC1392 over temperature.

In supply-voltage-monitor mode, the A/D makes a differential measurement between the 2.42V reference and the actual power-supply voltage. Each LSB step is approximately 4.727mV, giving a theoretical measurement range of 2.42V to 7.2V. The LTC1392 has guaranteed accuracy over a voltage range of 4.5V-6V, with a total absolute error of  $\pm 25\text{mV}$  or  $\pm 40\text{mV}$  over the commercial or industrial temperature range, respectively. To calculate voltage, use the formula  $(\text{ADC code} \times 4.727\text{mV}) + 2.42\text{V}$ .

The differential voltage input mode can be configured to operate in either 1V or 0.5V unipolar full-scale mode. Each mode converts the differential voltage between input pins  $+V_{IN}$  and  $-V_{IN}$  directly to bits, with the output code equal to  $[\text{ADC code} \times (\text{full scale}/1024)]$ . The 1V mode is specified at 8 bits accuracy, with the eighth bit accurate to  $\pm 1/2$  LSB or  $\pm 2\text{mV}$ , whereas

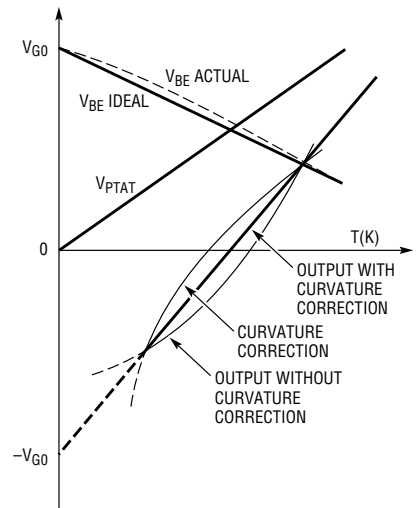


**Figure 3b. Output voltage versus temperature, showing curvature and curvature-corrected output**

the 0.5V full scale mode is specified to 7 bits accuracy  $\pm 1/2$  LSB, giving the same  $\pm 2\text{mV}$  accuracy. The differential inputs include a common-mode input range encompassing both power supply rails, allowing them to be used to measure the voltage across a sense resistor in either leg of the power supply. They can also be used to make a unipolar differential transducer bridge measurement, or to make a single-ended voltage measurement by grounding the  $-V_{IN}$  pin.

The LTC1392's three- or four-wire serial interface allows it to fit into an 8-pin SO or DIP package, and makes connection to virtually any microprocessor easy. Four pins are dedicated to the serial interface: active-low chip select (CS), clock (CLK), data input ( $D_{IN}$ ), and data output ( $D_{OUT}$ ). The  $D_{IN}$  pin is used to configure the LTC1392

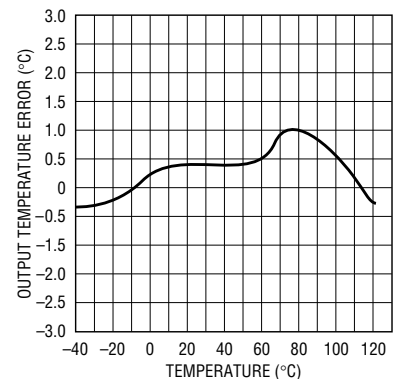


**Figure 4. Sensor error versus temperature (temperature output)**

for the measurement, and the D<sub>OUT</sub> pin outputs the A/D conversion data. The D<sub>IN</sub> pin is disabled after a valid configuration word is received, and the D<sub>OUT</sub> pin is in three-state mode until a valid configuration word is recognized, allowing the two pins to be tied together in a three-wire system. The serial link allows several devices to be attached to a common serial bus, with separate  $\overline{CS}$  lines to select the active chip. The small size and low pin count make the LTC1392 useful in compact, remotely located systems, or in isolated systems with a limited number of control wires. The 350 $\mu$ A current consumption and 1 $\mu$ A shutdown mode make it usable in low-power or battery-operated systems, and single-supply operation eliminates the need for a negative supply voltage.

## Typical Application

Figure 5 shows a typical LTC1392 application. A single-point "star" ground is used along with a ground plane to minimize errors in the volt-

age measurements. The power supply is bypassed directly to the ground plane with a 1 $\mu$ F tantalum capacitor in parallel with an 0.1 $\mu$ F ceramic capacitor.

The conversion time is set by the frequency of the signal applied to the CLK pin. The conversion starts when the  $\overline{CS}$  pin goes low. The falling edge of  $\overline{CS}$  signals the LTC1392 to wake up from micropower shutdown mode. After the LTC1392 recognizes the wake-up signal, it requires an additional 80 $\mu$ s delay for a temperature measurement, or a 10 $\mu$ s delay for a voltage measurement, followed by a 4-bit configuration word shifted into D<sub>IN</sub> pin. This word configures the LTC1392 for the selected measurement and initiates the A/D conversion cycle. The D<sub>IN</sub> pin is then disabled and the D<sub>OUT</sub> pin switches from three-state mode to an active output. A null bit is then shifted out of the D<sub>OUT</sub> pin on the falling edge of the CLK, followed by the result of the selected conversion. The output data can be formatted as an MSB-first sequence

or as an MSB-first followed by an LSB-first sequence, providing easy interface to either LSB-first or MSB-first serial ports. The minimum conversion time for the LTC1392 is 142 $\mu$ s in temperature mode or 72 $\mu$ s in the voltage-conversion modes, both at the maximum clock frequency of 250kHz.

## Conclusion

The LTC1392 provides a versatile data acquisition and environmental monitoring system with an easy-to-use interface. Its low supply current, coupled with space-saving SO8 or DIP packaging, makes the LTC1392 ideal for systems that require temperature, voltage, and current measurement while minimizing space, power consumption, and external component count. The combination of temperature- and voltage-measurement capability on one chip makes the LTC1392 unique in the market, providing the smallest, lowest power multifunction data acquisition system available.  $\blacktriangleleft$

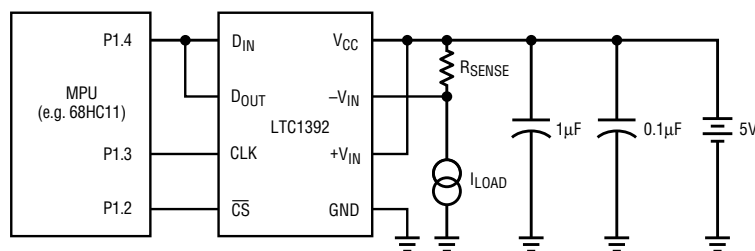


Figure 5. Typical LTC1392 application

# LT1580 Low-Dropout Regulator Uses New Approach to Achieve High Performance

by Craig Varga

## Introduction

Low-dropout regulators have become more common in desktop computer systems as microprocessor manufacturers have moved away from 5V-only CPUs. A wide range of supply requirements exist today, with new voltages just over the horizon. In many cases, the input-output differential is very small, effectively disqualifying many of the low-dropout regulators on the market today. Several manufacturers have chosen to achieve lower dropout by using PNP-based regulators. The drawbacks of this approach include much larger die size, inferior line rejection, and poor transient response.

## Enter the LT1580

The new LT1580 NPN regulator is designed to make use of the higher supply voltages already present in most systems. The higher voltage source is used to provide power for the control circuitry and supply the drive current to the NPN output transistor. This allows the NPN to be driven

into saturation, thereby reducing the dropout voltage by a  $V_{BE}$  compared to a conventional design. Applications for the LT1580 include 3.3V to 2.5V conversion with a 5V control supply, 5V to 4.2V conversion with a 12V control supply, or 5V to 3.6V conversion with a 12V control supply. It is easy to obtain dropout voltages as low as 0.4V at 4A, along with excellent static and dynamic specifications.

The LT1580 is capable of 7A maximum, with approximately 0.8V input-to-output differential. The current requirement for the control voltage source is approximately 1/50 of the output load current, or about 140mA for a 7A load. The LT1580 presents no supply-sequencing issues. If the control voltage comes up first, the regulator will not try to supply the full load demand from this source. The control voltage must be at least 1V greater than the output to obtain optimum performance. For adjustable regulators, the adjust-pin current is approximately 60 $\mu$ A and

varies directly with absolute temperature. In fixed regulators, the ground pin current is about 10mA and stays essentially constant as a function of load. Transient response performance is similar to that of the LT1584 fast-transient-response regulator. Maximum input voltage from the main power source is 7V, and the absolute maximum control voltage is 14V. The part is fully protected from over-current and over-temperature conditions. Both fixed voltage and adjustable versions are available. The adjustables are packaged in 5-pin TO-220s, whereas the fixed-voltage parts are 7-pin TO-220s.

## The LT1580 Brings Many New Features

Why so many pins? The LT1580 includes several innovative features that require additional pins. Both the fixed and adjustable versions have remote-sense pins, permitting very accurate regulation of output voltage at the load, where it counts, rather than at the regulator. As a result, the typical load regulation over a range of 100mA to 7A with a 2.5V output is approximately 1mV. The sense pin and the control-voltage pin, plus the conventional three pins of an LDO regulator, give a pin count of five for the adjustable design. The fixed-voltage part adds a ground pin for the bottom of the internal feedback divider, bringing the pin count to six. The seventh pin is a no-connect.

Note that the adjust pin is brought out even on the fixed-voltage parts. This allows the user to greatly improve the dynamic response of the regulator by bypassing the feedback divider with a capacitor. In the past, using a fixed regulator meant suffering a loss of performance due to lack of such a bypass. A capacitor value of

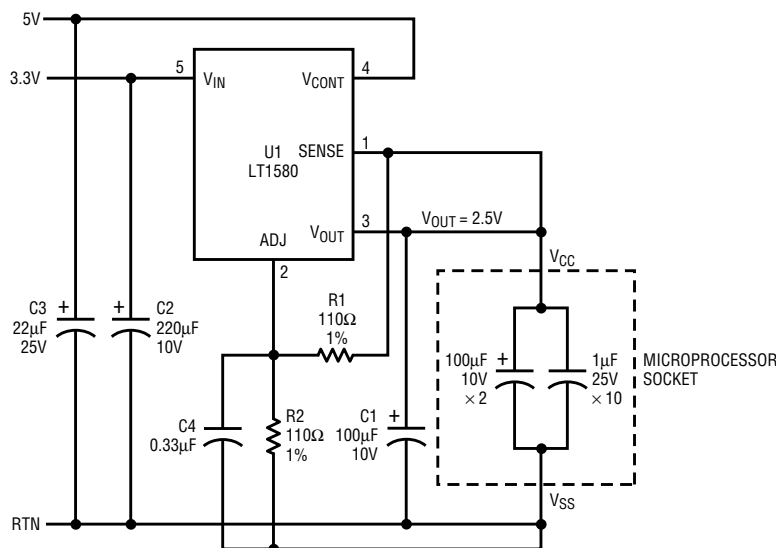
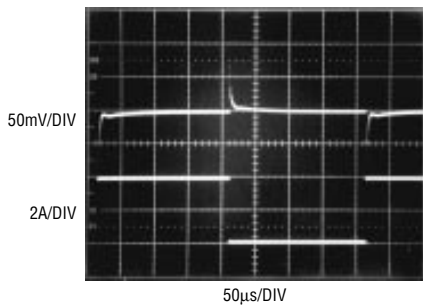
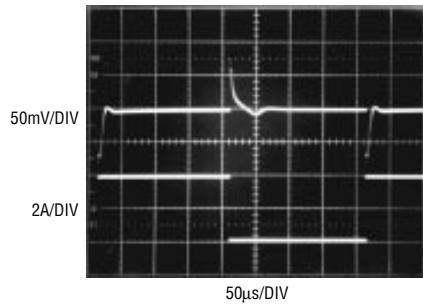


Figure 1. LT1580 delivers 2.5V from 3.3V at up to 6A



**Figure 2. Transient response of Figure 1's circuit with adjust-pin bypass capacitor. Load step is from 200mA to 4A**



**Figure 3. Transient response without adjust-pin bypass capacitor. Otherwise, conditions are the same as in Figure 2**

0.1µF to approximately 1µF will generally provide optimum transient response. The value chosen depends on the amount of output capacitance in the system. Although the capacitor's final value is empirically determined, it generally increases as the output capacitance increases.

In addition to the enhancements already mentioned, the reference accuracy has been improved by a factor of two, with a guaranteed 0.5% tolerance. Temperature drift is also very well controlled. The part uses ratiometrically accurate internal divider resistors. The part can easily hold 1% output accuracy over temperature, guaranteed, while

operating with an input/output differential of well under 1V.

In some cases, a higher supply voltage for the control voltage will not be available. If the control pin is tied to the main supply, the regulator will still function as a conventional LDO and offer a dropout specification approximately 70mV better than conventional NPN-based LDOs. This is the result of eliminating the voltage drop of the on-die connection to the control circuit that exists in older designs. This connection is now made externally, on the PC board, using much larger conductors than are possible on the die.

## Circuit Examples

Figure 1 shows a circuit designed to deliver 2.5V from a 3.3V source with 5V available for the control voltage. Figure 2 shows the response to a load step of 200mA to 4.0A. The circuit is configured with a 0.33µF adjust-pin bypass capacitor. The performance without this capacitor is shown in Figure 3. This difference in performance is the reason for providing the adjust pin on the fixed-voltage devices. A substantial savings in expensive output decoupling capacitance may be realized by adding a small "1206-case" ceramic capacitor at this pin.

Figure 4 shows an example of a circuit with shutdown capability. By switching the control voltage rather than the main supply, the transistor providing the switch function needs only a small fraction of the current handling ability that it would need if it was switching the main supply. Also, in most applications, it is not necessary to hold the voltage drop across the controlling switch to a very low level to maintain low-dropout performance.

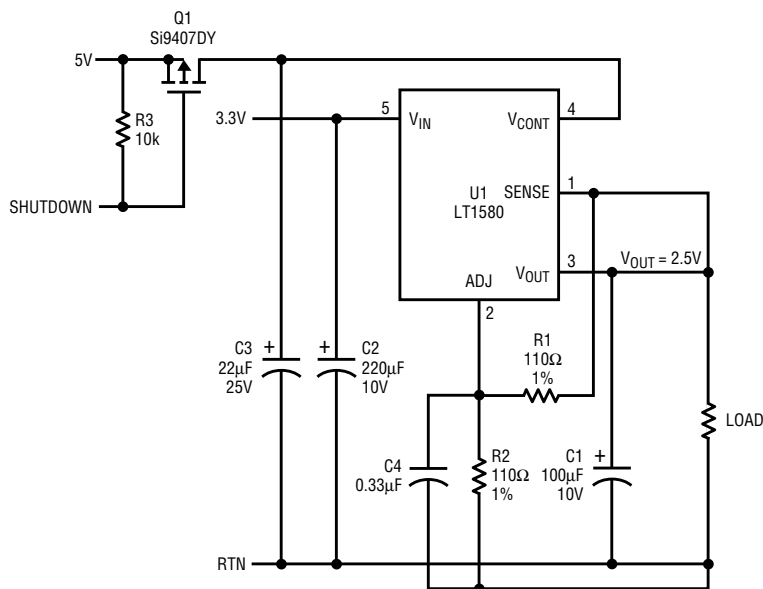


**Figure 4. Small FET adds shutdown capability to LT1580 circuit**

# Quad Current-to-Voltage Converter is Ideal for Optical Disk Drives

by William H. Gross

## Introduction

The LT1311 is a quad current-to-voltage converter designed for the demanding requirements of photodiode amplification. A new approach to current-to-voltage conversion provides excellent DC and AC performance without external DC trims or AC frequency compensation. The LT1311 is ideal for converting multiple photodiode currents to voltages, and for general purpose, matched inverting-amplifier applications. Figure 1 shows the LT1311 pin configuration and a typical photodiode amplifier application.

The LT1311 has the excellent speed and power performance of a current-feedback amplifier with the DC accuracy and low noise of a voltage-feedback amplifier. The internal feedback resistor is 20k, resulting in a current-to-voltage gain of 20mV/ $\mu$ A. The -3dB bandwidth is 12MHz and settling time is less than 145ns to 0.1% of final value for a 2V output step. The four amplifiers draw only 7mA of supply current while operating on all supplies from  $\pm$ 2V (4V total) to  $\pm$ 15V (30V total). The input-referred bias current is typically 75nA and drift is less than 0.5nA/ $^{\circ}$ C. The input noise is only 5pA/ $\sqrt{\text{Hz}}$ . Table 1 details the LT1311 performance.

## Optical Disk Drives

There are many types of optical data storage. All have one thing in common: the amount of light reflected off the storage medium indicates whether a given data bit is a "one" or a "zero." The detection of the reflected light requires a photo detector, the most common of which is the photo diode. The current that flows through a photo diode is proportional to the amount of light incident on the diode. Optical disk drives usually use a single-chip array of four to eight photo diodes. These matched photo

diodes provide both position and intensity information to the servo systems that keep the laser focused, on track, and at the correct output level.

In read-only optical drives, such as audio CD players and CD ROM drives, the laser level is constant and the amount of reflected light is not critical. This, combined with the extensive data conditioning done before recording, allows automatic gain control and AC coupling of the photodiode signals. The amplifiers that

convert these photodiode currents to useful signals do not require good DC precision.

Optical drives that record and play, such as magneto-optical and phase-change drives, require tight control of the laser output level. This is because a high level of laser output is used to write and a much lower level is used to read the data. These drives also need to record quickly, limiting the amount of data conditioning that can be done before recording. The

Table 1. LT1311 electrical characteristics

$V_{CC} = 10V$ ,  $V_{EE} = \text{Ground}$ , Bias = 5V,  $T_A = 0^{\circ}\text{C} - 70^{\circ}\text{C}$  unless otherwise stated.

| Parameter   | Min      | Typ       | Max       | Units                  |
|---|----------|-----------|-----------|------------------------|
| Current to Voltage Gain   | 19.2     | 20        | 20.8      | mV/ $\mu$ A            |
| Current to Voltage Gain Drift   |          | -70       |           | ppm/ $^{\circ}$ C      |
| Current to Voltage Gain Mismatch                                      |          | 0.1       |           | %                      |
| Input Offset Voltage  |          | $\pm$ 150 | $\pm$ 500 | $\mu$ V                |
| Input Offset Voltage Drift  |          | $\pm$ 1   |           | $\mu$ V/ $^{\circ}$ C  |
| Inverting Input Current   |          | 75        | 250       | nA                     |
| Inverting Input Current Drift   |          | 0.5       | 2.5       | nA/ $^{\circ}$ C       |
| Output Offset Voltage   |          | 1.5       | 5         | mV                     |
| Output Offset Voltage Drift   |          | 10        | 50        | $\mu$ V/ $^{\circ}$ C  |
| Output Noise Voltage Density, 1kHz                                    |          | 100       |           | nV/ $\sqrt{\text{Hz}}$ |
| Input Noise Current Density, 1kHz                                     |          | 5         |           | pA/ $\sqrt{\text{Hz}}$ |
| Input Noise Voltage Density, 1kHz                                     |          | 4.5       |           | nV/ $\sqrt{\text{Hz}}$ |
| Input Resistance  |          | 0.2       | 2         | $\Omega$               |
| Input Impedance, 10MHz  |          | 300       |           | $\Omega$               |
| Power Supply Rejection Ratio, $V_s = \pm 2$ to $\pm 15V$<br>Bias = 0V | 90       | 103       |           | dB                     |
| Maximum Output Swing  |          |           |           |                        |
| Output High, No Load  | 8.8      | 9.0       |           | V                      |
| Output High, 10mA Load  | 8.5      | 8.8       |           | V                      |
| Output Low, No Load   |          | 1.0       | 1.2       | V                      |
| Output Low, 10mA Load   |          | 1.2       | 1.5       | V                      |
| Maximum Output Current  | $\pm$ 30 | $\pm$ 55  |           | mA                     |
| Total Quiescent Supply Current  |          | 7         | 11        | mA                     |
| Slew Rate   |          | 80        |           | V/ $\mu$ s             |
| Small Signal Bandwidth  |          | 12        |           | MHz                    |
| Rise and Fall Time  |          | 35        |           | ns                     |
| Settling Time, 0.1% of 2V Step  |          | 145       |           | ns                     |

photodiode signals must be DC coupled into a wide dynamic range system. The amplifiers that convert these photodiode currents to useful signals require excellent DC and AC performance.

For more details on optical disk drives, please read the excellent article by Praveen Asthana, entitled "A Long Road to Overnight Success," in the October, 1994 issue of *IEEE Spectrum*.

**Photodiode Amplifier Requirements**

The read-write optical disk drive requires a fast photodiode current-to-voltage converter with very good DC accuracy. The bandwidth of the converter needs to be greater than 10MHz and the output must settle to

within 0.5% of the final value in less than 200ns for a 100µA input step. The output current of the photo diodes ranges from about 1µA to 100µA; a conversion gain of 20mV/µA results in an output signal of 2V peak-to-peak, which is easy to handle on a single 5V or 10V supply. The initial offset errors of the photo diodes and converters are easily trimmed out at room temperature; however, the input-referred offset drift of the current-to-voltage converter must not exceed 10% of the minimum input signal. For a 1µA input and a 40°C maximum change in operating temperature, the converter must have an input-referred offset drift of less than 2.5nA/°C. Hence, for a 20mV/µA conversion gain, the output offset voltage drift must be less than 50µV/°C. Additionally, there is a physical size constraint: four complete converters in a small, surface-mount package would be ideal for mounting close to the diode array.

**Traditional Solutions**

Most photodiode current-to-voltage converters use the inverting amplifier circuit of Figure 2. The 20mV/µA conversion gain implies a 20k feedback resistor. Diode capacitance and/or stray capacitance of just 5pF combined with a 20k resistor results in a pole at 1.6MHz. To move the pole out to a higher frequency, a smaller resistor can be used, but the lost gain must be made up somewhere. The additional voltage gain would cause more output offset drift. Operating the amplifier at unity gain gives the best DC performance. With a 20k feedback resistor, the pole due to the diode capacitance must be canceled by the feedback capacitor in order to use a fast op amp. This cancellation must be quite accurate in order to get fast output settling. The diode and stray capacitance are not well controlled and the worst case settling time is determined by the mismatch in the pole-zero cancellation.

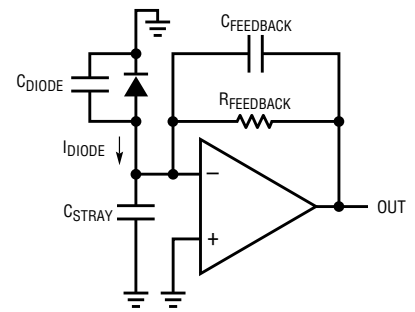


**Figure 2. Inverting op amp I-to-V converter**

**Current-Feedback Photodiode Amplifiers**

If a current-feedback amplifier is used for the op amp in Figure 2, the feedback capacitor becomes unnecessary. To understand why, refer to the simplified schematic of a current-feedback amplifier in Figure 3. The inverting input of the amplifier is the junction of the emitters of Q3 and Q4, and therefore a low impedance. The pole formed by the capacitance at the inverting input is usually many times higher than the bandwidth of the amplifier, and therefore has almost no effect on settling time. Using a current-feedback amplifier eliminates the need to cancel the diode capacitance. For example, adding 50pF to the input of the LT1311 only increases the settling time by a factor of two. This makes it feasible to locate the

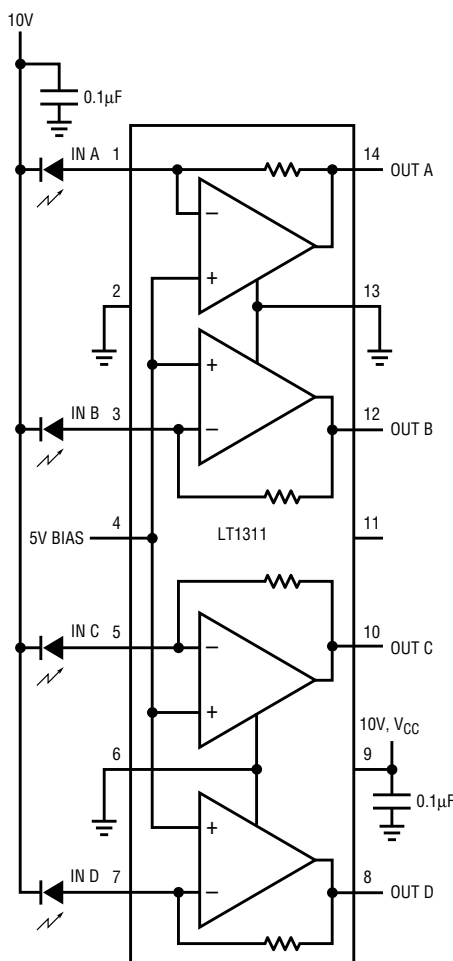


**Figure 1. Photodiode current-to-voltage converter**

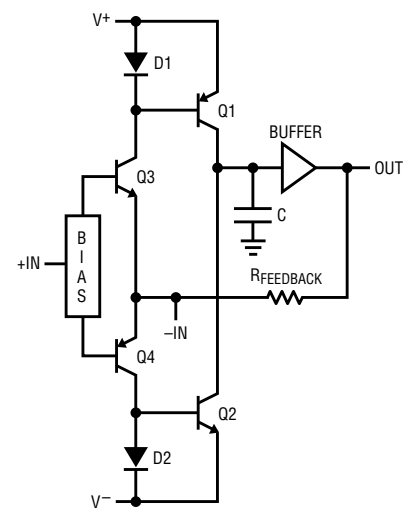


**Figure 3. Basic current-feedback amplifier**

amplifier a short distance away from the photo diodes.

The bandwidth of a current-feedback amplifier is determined by the feedback resistor and the internal compensation capacitor. Hence, if the feedback resistor that gives the desired gain also gives the desired bandwidth, everything is OK. Unfortunately, most commercial CFAs are optimized for feedback resistors of 1k or less in order to make stray capacitance less of a problem. For example, if we use an LT1217 or LT1223 with a 20k feedback resistor, the bandwidth will be less than 2MHz. In addition to the low bandwidth problem, there is a problem with inverting-input bias-current drift. Even the low-current LT1217, with its guaranteed input bias current of less than 500nA, cannot guarantee less than 2.5nA/°C of bias current drift. In order to take advantage of the AC performance of current feedback, an improvement to the LT1217 circuit is required.

### The Current Feedback Circuit

Referring to the basic current-feedback amplifier schematic in Figure 3, we see that the error current that flows in the feedback resistor is mirrored by D1/Q1 and by D2/Q2 before it goes to the compensation capacitor. For a given bandwidth, increasing the gain of the current mirrors D1/Q1 and D2/Q2 increases the size of the feedback resistor. In the 12MHz LT1311, the mirror has a gain of three, the compensation capacitor is 2pF, and the feedback resistor is 20k.

Again referring to Figure 3, we can look for the sources of DC error. The input offset voltage (and drift) of this amplifier can be very low with the proper biasing; however, the inverting input bias current is hard to control because it is the difference between the emitter currents of Q3 and Q4. There are three things that generate inverting input bias current: the mismatch in the alphas of Q3 and Q4, the mismatch in the gains of current mirrors D1/Q1 and D2/Q2, and the input bias current of the output buffer.

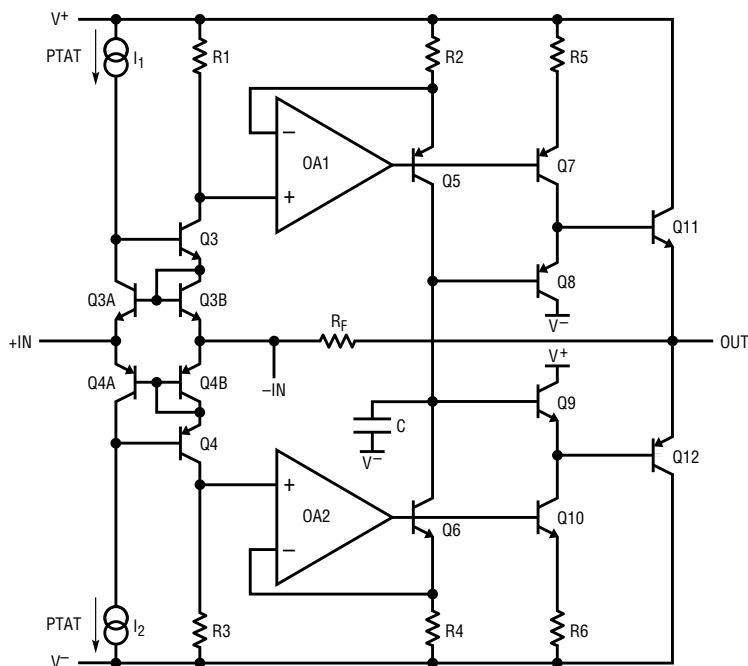


Figure 4. LT1311 circuit concept

### The LT1311 Circuit

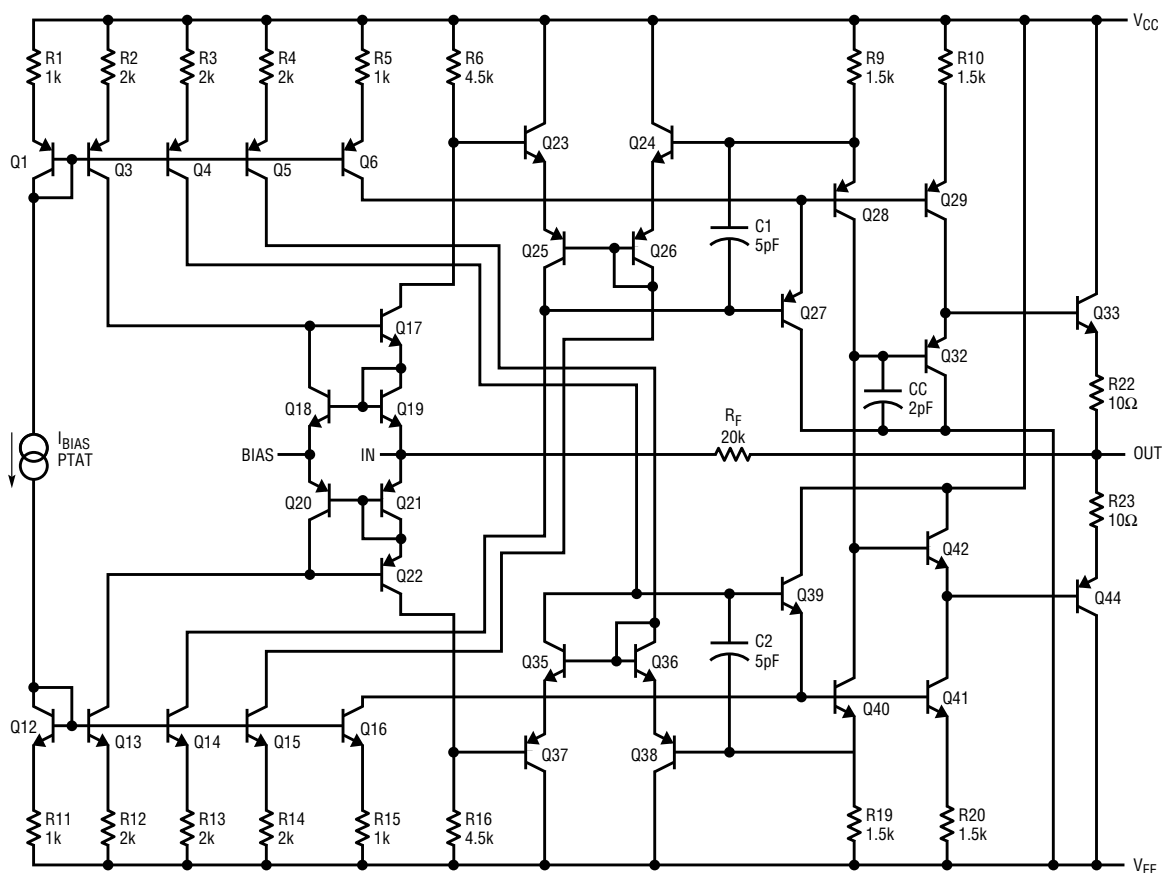
In the basic LT1311 circuit of Figure 4, two current sources and Wilson mirrors are used as the bias for the input transistors Q3 and Q4. In this circuit the alpha errors are eliminated (first-order) and only the alpha matching between similar types of transistors generates an inverting input bias current. In a typical IC process, the beta matching of identical transistors is better than 5%. If Q3 and Q3B have a beta mismatch of 5% and all the other transistors are perfectly matched, the inverting input bias current is 0.024% of the collector currents. This small current is less than the other sources of input bias current. The current mirrors are the largest source of DC errors in a current-feedback amplifier and the LT1311 dramatically improves the mirrors.

Figure 4 shows the basic idea of replacing the D1/Q1 current mirror with R1, R2, OA1, and Q5 and similarly replacing D2/Q2 with R3, R4, OA2, and Q6. There are three sources of input bias current due to this new current mirror. The first results from the difference in the ratio of R1:R2 and R3:R4. Note that the absolute value of this ratio does not generate

any input bias current. In standard IC processes with thin-film resistors, the resistor ratio matching is better than 0.1%.

The next source of input bias current in this new mirror is the difference in input offset voltage between OA1 and OA2. The magnitude of this current is the difference in the two op amps' offset voltages divided by R1. In a typical IC process, the op amp offsets will match within 2mV, and a typical voltage drop across R1 would be 200mV; therefore the input bias current due to OA1/OA2 mismatch would be 1% of the collector current. This is ten times larger than the contribution due to the resistor-ratio mismatch.

The last source of input bias current in the mirrors is the alpha mismatch of Q5 and Q6. The alpha errors of Q5 and Q6 are canceled (first-order) by the base currents of Q8 and Q9. Therefore, only the mismatch in current gain between two similar transistors causes input bias current. For a typical beta of 200, with a worst-case beta mismatch of 5%, the input bias current would be 0.02% of the collector current, so this contribution is very small.



**Figure 5. Simplified schematic of one LT1311 amplifier**

In summary, the new op amp-based mirror reduces the inverting-input bias current to about 1% of the collector current, making it comparable to the input bias current of a voltage-feedback op amp. More importantly, the drift of the input bias current is very predictable. Mismatch in resistor ratios generates an input bias current that has the same temperature coefficient as the collector currents of Q3 and Q4. The op amp offsets generate bias current with a temperature coefficient of exactly  $\Delta V_{BE}$  divided by resistance. This is often called "proportional-to-absolute temperature," or "PTAT." If the collector current in Q3 and Q4 is also PTAT, then the drift of the inverting input bias current will be PTAT.

If the offset voltage of one of the op amps in one of the mirrors is adjusted until the inverting-input bias current is zero, the current will stay at zero because both op amps'  $V_{OS}$  have the same drift: PTAT. This is very

powerful, because it is not necessary to actually know the offset of OA1 or OA2 in order to eliminate the drift they cause; it is only necessary to trim their offsets so that the inverting-input bias current is zero.

In the simplified schematic of the LT1311 (Figure 5), we can see how all of this comes together. All four amplifiers on the chip are complete and identical; only the supplies and the noninverting inputs are common. The main bias current source,  $I_{BIAS}$ , which is used to generate source and sink current sources for the rest of the circuitry, is PTAT. Q23–Q27 and C1 make up the signal portion of op amp OA1, and Q14, R13, Q15, R14, Q6, and R5 make up the bias portion of OA1. Similarly Q35–Q39 and C2 make up the signal portion of OA2 whereas Q4, R3, Q5, R4, Q16, and R15 make up the bias portion of OA2. As mentioned earlier, the LT1311 current mirrors have a gain of three, set by R6 and R9 (R16 and R19). This

allows a 2pF compensation capacitor to work with the 20k feedback resistor to set a 12MHz bandwidth.

The thin-film resistors in the biasing circuitry of each amplifier are laser trimmed at wafer sort. The offset voltage of OA1 is trimmed in one direction by R13 and in the other direction by R14. Similarly, R3 and R4 trim the offset of OA2. The amplifier input offset voltage is trimmed in one direction by R1 and in the other direction by R11. The 20k feedback resistor is trimmed to set the gain.

The four current-feedback amplifiers are packaged in a 14-pin SO package with a nonstandard pinout. The four inverting inputs are on one side of the package; the inputs are separated by DC supply or bias pins for optimum channel separation. The noninverting inputs are tied to a common bias point and the outputs are on the other side of the package for minimum output-to-input coupling.

*continued on page 21*

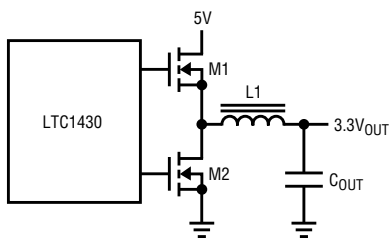


Figure 1. Functional block diagram, LTC1430 circuit architecture

continued from page 1

MOSFETs. The on-chip output drivers feature separate power-supply inputs and internal level shifters, allowing the MOSFET gate drive to be tailored for logic-level or standard threshold devices. The stepped-up gate drive to M1 can be generated with a simple charge-pump scheme (Figure 2a), or it can be provided by a low-power, higher-voltage supply if one is available (Figure 2b). Low on-resistance MOSFETs can be used to minimize dissipation even at high current levels; this maximizes efficiency in power-conscious designs and allows the elimination of the heat sink in many cases.

External component count in the high-current path is minimized by eliminating low-value current-sense resistors. Voltage feedback eliminates the need for current sensing under normal operating conditions, and output current limit is sensed by monitoring the voltage drop across the  $R_{DS\ ON}$  of M1 during its ON state. Current limit is set by specifying the  $R_{DS\ ON}$  of M1 and setting the maximum voltage allowed with a single external resistor at the  $I_{MAX}$  pin (Figure 3). Current limit can also be disabled if desired by tying the  $I_{MAX}$  pin to ground. The current-limit circuit is designed to engage slowly under mild transient overloads and to kick in more quickly to prevent component damage under severe overcurrent and short-circuit conditions. Current-limit recovery time is set by the external soft start capacitor, providing a controlled return to full output voltage after the fault is removed.

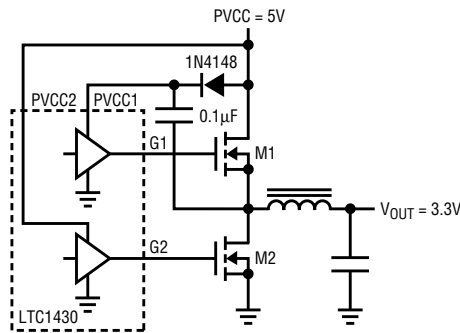


Figure 2a. Gate drive using 5V supply

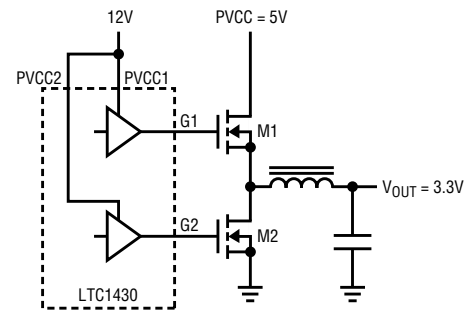


Figure 2b. Gate drive using 5V and 12V supplies

### Performance Features

The LTC1430 uses a voltage feedback loop to control output voltage. It includes two additional “safety belt” internal feedback loops to improve high-frequency transient response (Figure 4). The MAX loop responds within a single clock cycle when the output exceeds the set point by more than 3%, forcing the duty cycle to 0% and holding M2 on continuously until the output drops back into the acceptable range. Similarly, the MIN loop kicks in when the output sags 3% below the set point, forcing the LTC1430 to 90% duty cycle until the output recovers. The 90% maximum ensures that charge-pump drive continues to be supplied to the top MOSFET driver, preventing the gate drive to M1 from deteriorating during extended transient loads. The MAX feedback loop is always active, providing a measure of protection even

if the 5V input supply is accidentally shorted to the lower microprocessor supply. Under this condition, M2 will crowbar the low supply to ground through the inductor until the main supply fuse blows or the higher supply goes into current limit. The MIN loop is disabled at start-up or during current limit to allow soft start to function and to prevent MIN from taking over when the current-limit circuit is active.

The LTC1430 includes an onboard reference trimmed to  $1.265V \pm 10mV$  and an onboard 0.1% resistor-divider string that provides a fixed 3.3V output. External resistors can be used to generate other output voltages. Note that a pair of 1% resistors will add 2% to the output-error budget; 0.1% resistors are recommended for applications that require very tight

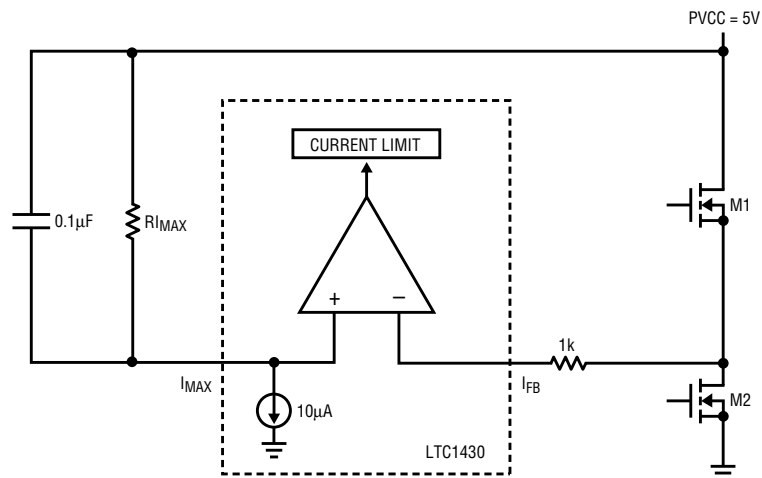
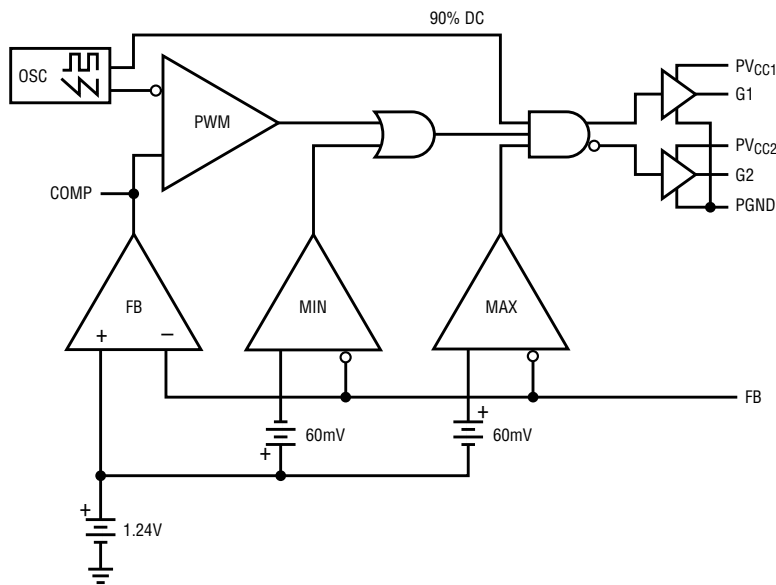


Figure 3. One resistor sets current limit on the LTC1430



**Figure 4. Two additional feedback loops improve the transient response of the LTC1430**

### A Typical 5V-to-3.3V Application

The typical application for the LTC1430 is a 5V-to-3.3V converter on a PC motherboard. The output is used to power a Pentium, P6, or similar class processor, and the input is taken from the system 5V  $\pm 5\%$  supply. The LTC1430 provides the precisely regulated output voltage required by the processor without the need for an external precision reference or trimming. Figure 5 shows a typical application with a 3.30V  $\pm 1\%$  output voltage and a 12A output-current limit. The power MOSFETs are sized so as not to require a heat sink under ambient temperature conditions up to 50°C. Typical efficiency is above 91% from 1A to 10A output current, and peaks at 95% at 5A (Figure 6).

The 12A current limit is set by the 16k resistor R1 from PV<sub>CC</sub> to I<sub>MAX</sub>, and the 0.035Ω on-resistance of the MTD20N03HL MOSFETs (M1a, M1b).

output tolerances. The LTC1430 specifies load regulation of  $\pm 15\text{mV}$  and line regulation of  $\pm 3\text{mV}$ , resulting in a total worst-case output error of  $\pm 1.6\%$  when used with the internal divider or 0.1% external resistors. The internal reference will drift an additional  $\pm 5\text{mV}$  over the 0°C–70°C temperature range, providing a  $\pm 2.0\%$  total error budget over this temperature range.

The LTC1430 includes a versatile internal oscillator that can be set to free run at any frequency between 100kHz and 500kHz, or synchronized to an external clock signal. The oscillator runs at a nominal 200kHz frequency with the FREQ pin floating. An external resistor from FREQ to ground will speed up the internal oscillator, up to a maximum operating frequency of 500kHz; a resistor to V<sub>CC</sub> will slow the oscillator to below 100kHz. The internal oscillator can be synchronized to an external clock signal by setting the free-running frequency to slightly slower than the synchronizing clock frequency and applying the clock signal to the  $\overline{\text{SD}}$  pin. The LTC1430 will shut down only if the  $\overline{\text{SD}}$  pin is low continuously for more than 50μs. In shutdown mode, the power-supply current drawn by the LTC1430 drops to below

1μA. When the shutdown pin is brought high again, the LTC1430 will run through a soft start cycle and resume normal operation.

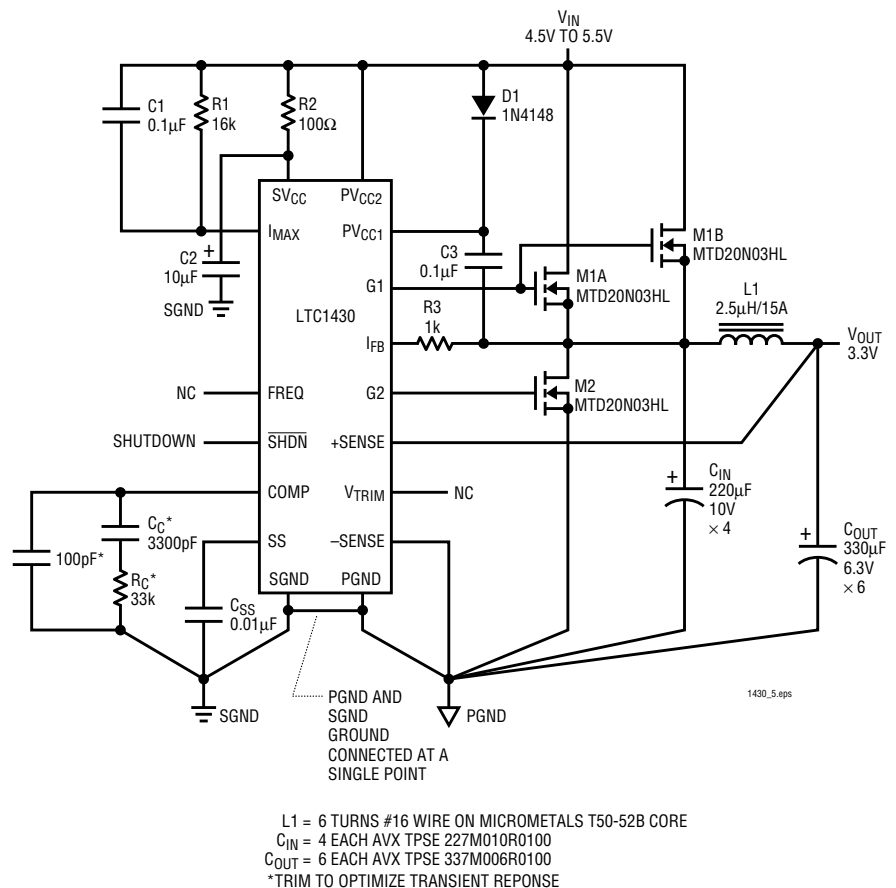


**Figure 5. Typical 5V-to-3.3V, 10A LTC1430 application**

L1 = 6 TURNS #16 WIRE ON MICROMETALS T50-52B CORE  
 C<sub>IN</sub> = 4 EACH AVX TPSE 227M010R0100  
 C<sub>OUT</sub> = 6 EACH AVX TPSE 337M006R0100  
 \*TRIM TO OPTIMIZE TRANSIENT REPONSE

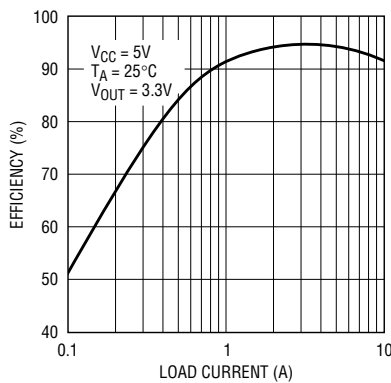


**Figure 6. Efficiency plot for Figure 5's circuit. Note that efficiency peaks at a respectable 95%**

The 0.1 $\mu$ F capacitor in parallel with R1 improves power-supply rejection at  $I_{MAX}$ , providing consistent current-limit performance when voltage spikes are present at  $PV_{CC}$ . Soft start time is set by  $C_{SS}$ ; the 0.01 $\mu$ F value shown reacts with an internal 10mA pull-up to provide a 3ms start-up time. The 2.5 $\mu$ H, 15A inductor is sized to allow the peak current to rise to the full current-limit value without saturating. This allows the circuit to withstand extended output short circuits without saturating the inductor core. The inductor value is chosen as a compromise between peak ripple current and output-current slew rate, which affects large-signal transient response. If the output load is expected to generate large output-current transients (as large microprocessors

tend to do), the inductor value will need to be quite low, in the 1 $\mu$ H–10 $\mu$ H range.

Loop compensation is critical for obtaining optimum transient response with a voltage-feedback system like the LTC1430; the compensation components shown here give good response when used with the output capacitor values and brands shown (Figure 7). The ESR of the output capacitor has a significant effect on the transient response of the system. For best results, use the largest value, lowest ESR capacitors that will fit the design budget and space requirements. Several smaller capacitors wired in parallel can help reduce total output capacitor ESR to acceptable levels. Input bypass capacitor ESR is also important to keep input supply variations to a minimum with 10A<sub>p-p</sub> square-wave current pulses flowing into M1. AVX TPS-series surface-mount tantalum capacitors and Sanyo OS-CON organic electrolytic capacitors are recommended for both input and output bypass duty. Low cost "computer grade" aluminum electrolytics typically have much higher series resistance and will significantly degrade performance. Don't count on that parallel 0.1 $\mu$ F ceramic cap to lower the ESR of a cheap electrolytic cap to acceptable levels.

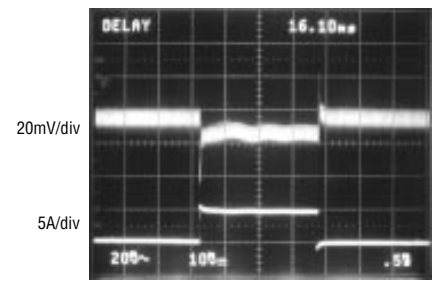


**Figure 7. Transient response: 0A-to-5A load step imposed on Figure 5's output**

### Conclusion

The LTC1430 fits neatly into the power-supply niche created by the advent of new technology, power-supply-critical microprocessors. Its tight, no-trims output-voltage tolerance, and simple, low external-parts-count hookup make it a good fit on high-end PC motherboards or plug-in modules. Superior protection features, both for the power supply itself and for the circuitry connected to it, help maximize system reliability, especially in user-upgradable systems where unskilled screwdrivers are likely to be roaming around. High overall efficiency reduces the heat generated by the power supply, minimizing cooling and heat sinking requirements and reducing the power drawn by "green" systems. The design of the LTC1430, combined with Linear Technology's unparalleled applications support, simplifies the job of powering today's high performance microcomputers.

1311, continued from page 18

The output-to-input stray capacitance must be less than 0.5pF for proper settling performance; this pinout ensures that the input and output printed circuit board traces are far apart.

### Conclusion

The LT1311 is a new current-to-voltage converter that solves the optical disk drive photodiode amplifier problem with new circuit design, complementary bipolar processing, and laser trimming. The new circuit provides current-feedback AC per-

formance and low power consumption with the DC precision of voltage-feedback amplifiers. Other applications that require matched inverting amplifiers, such as color scanners, will also benefit from the LT1311's performance.

# Humidity Sensor to Data Acquisition System Interface

by Richard Markell

## Introduction

It can be difficult to interface humidity sensors to data acquisition systems because of the sensors' drive requirements and their wide dynamic range. By carefully selecting the de-

vices that comprise the analog front end, users can customize the circuit to meet their humidity-sensing requirements and achieve reasonable accuracy throughout the chosen range. This Design Idea details the analog front-end interface between a Phys-Chem Scientific Corp.<sup>1</sup> model EMD-2000 humidity sensor and a user selected (probably microprocessor-based) data acquisition system.

5 volts supply to -5 volts to supply power to U2, U3, and U4. U2A, part of an LTC1043 switched-capacitor building block, provides the excitation for the sensor, switching between 5 volts and -5 volts at a rate of approximately 2.2kHz. This rate can be varied, but we recommended that it be kept below approximately 2.4kHz, which is one-half the auto-zero rate of U3. We believe the deviation from the Phys-Chem response curves taken at 5kHz is insignificant.

## Design Considerations

The Phys-Chem humidity sensor is a small, low-cost, accurate resistance-type relative humidity (RH) sensor. This sensor has a well defined, stable response curve and can be replaced in circuit without system recalibration.

The design criteria call for a low-cost, high-precision analog front end that requires few calibration "tweaks" and operates on a single 5 volt supply. The sensor requires a square wave or sine wave excitation with no DC component. The sensor reactance varies over an extremely wide range (approximately 700Ω-20MΩ). The wide dynamic range (approximately 90dB) required to obtain the full RH range of the sensor results in some challenges for the designer.

The circuit shown in the schematic features zero-drift operational amplifiers (LTC1250 and LTC1050) and a precision instrumentation switched-capacitor block (LTC1043). This design will maintain excellent DC accuracy down to microvolt levels. This method was chosen over the use of a true RMS-to-DC or log converter because of the expense and temperature sensitivity of these parts.

## Circuit Description

Figure 1 is a schematic diagram of the circuit. Only a single 5 volt power supply is required. Integrated circuit U1, an LTC1046, converts the

Variable resistor R2 sets the full-scale output. Since the sensor resistance is 700Ω at approximately 90% humidity, setting R2 at 700Ω will provide a 2:1 voltage divider that, when combined with the gain of U4 (×2), results in an overall gain of one. U3 must be included in order for the circuit to function properly; otherwise C4 and C7 form a voltage divider that is dependent on the resistance of the RH sensor. U3 is a precision auto-zero operational amplifier with an auto-zero frequency of approximately 4.75kHz. U2B (the "lower" switch) samples the output of U3 and provides this sample to the input of U4. U4 is set to provide a gain of two.

It is easy to digitize the output of U4. Figure 2 is the schematic of a 12-bit converter that can be used for this purpose. The range of humidity that can be sensed depends on the resolution of the converter. The full-scale output (which is equivalent to approximately 90% humidity) is essentially independent of the number of bits in the A/D converter, but the dry (low RH) end of the scale is dependent on the A/D resolution. As an example, the above referenced 12-bit converter will process humidity signals that translate to approximately 20% RH, since the voltage output at this humidity is approximately 2.3 millivolts, while 1/2 LSB is 1.2 millivolts. Digitization down to 10% RH

### DESIGN IDEAS...

#### Humidity Sensor to Data Acquisition System Interface ..... 22

Richard Markell

#### Low-Power Signal Detection in a Noisy Environment . 24

Philip Karantzalis and Jimmylee Lawson

#### High Output-Current Boost Regulator ..... 26

Dimitry Goder

#### LT1111 Isolated 5V Switching Power Supply ..... 27

Kevin R. Hoskins

#### High-Efficiency EL Driver Circuit ..... 28

Dave Bell

#### Adding Features to the Boost Topology ..... 30

Dimitry Goder

#### Bandpass Filter Has Adjustable Q ..... 31

Frank Cox

#### Sallen and Key Filters Use 5% Values ..... 32

Dale Eagar

#### Simple Battery Charger Runs at 1MHz ..... 34

Mitchell Lee

#### Lithium-Ion Battery Charger ..... 35

Dimitry Goder

#### Three-Cell to 3.3V Buck-Boost Converter ... 36

Dimitry Goder

#### High Output-Voltage Buck Regulator ..... 37

Dimitry Goder

requires the conversion of 350µV signals or a 16-bit converter. From a cost standpoint this seems unwieldy. It is much more economical to use a two-channel 12-bit converter that changes ranges somewhere in the humidity range.

All of the above solutions measure output voltage from a voltage divider consisting of the RH sensor and a fixed "calibration" resistor. The resistance of the sensor at a fixed output

voltage can be calculated from the formula

$$R \text{ (Ohms)} = \frac{R2 V_{\text{FULL SCALE}}}{V_{\text{OUT}}/2} - R2$$

In this case, if R2 is set to 700 ohms, and  $V_{\text{FULL SCALE}} = 5.00\text{V}$ , then

$$R \text{ (Ohms)} = \frac{3500}{V_{\text{OUT}}/2} - 700$$

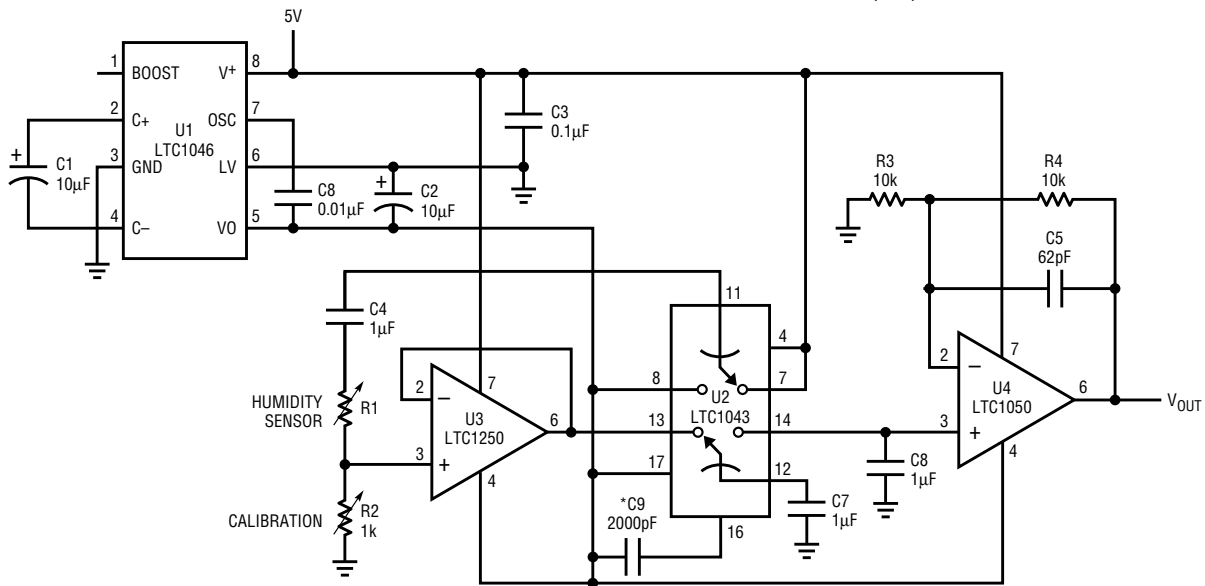
Once R is calculated (probably by the microprocessor), the humidity can

be calculated from the quadratic approximation in the Phys-Chem literature:

$$RH = \text{Ln}R - 14.06 - \frac{\sqrt{(14.06 - \text{Ln}R)^2 + 15.56}}{-0.176}$$

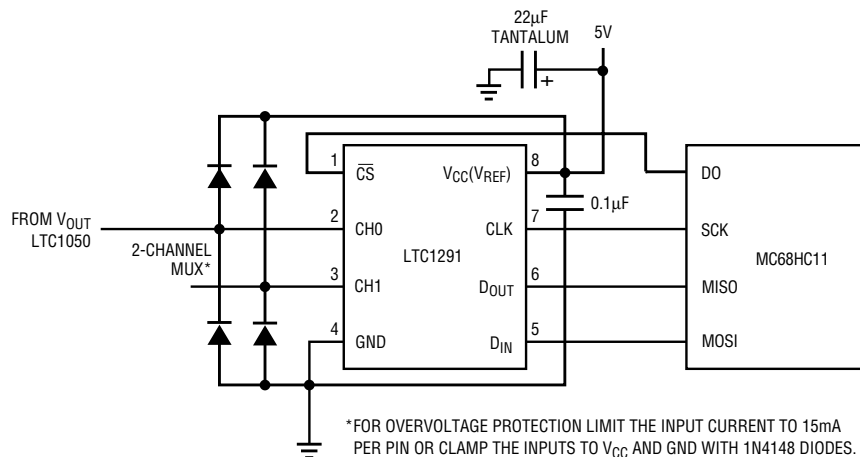
If a suitable humidity chamber is not available, the sensor can be removed and fixed resistors substituted. The circuit should then be calibrated from the EMD-2000 "typical response curve." This should provide approximately 2% accuracy. 

1. Phys-Chem Scientific Corp.  
36 West 20th Street  
New York, NY 10011  
(212) 924-2070—Phone  
(212) 243-7352—FAX



NOTES: UNLESS OTHERWISE SPECIFIED  
1. ALL RESISTANCES ARE IN OHMS, 1/4 W 5%  
\*C9 ADJUSTS OSC. FREQUENCY 2000pF YIELDS ~ 2.2kHz

Figure 1. Schematic diagram of humidity-sensor circuit



\*FOR OVERVOLTAGE PROTECTION LIMIT THE INPUT CURRENT TO 15mA PER PIN OR CLAMP THE INPUTS TO VCC AND GND WITH 1N4148 DIODES.

Figure 2. LTC1291 12 bit A/D converter interfaced to MC68HC11

# Low-Power Signal Detection in a Noisy Environment

by Philip Karantzalis and Jimmylee Lawson

## Introduction

In signal-detection applications where a small narrowband signal is to be detected in the presence of wideband noise, one can design an asynchronous (non-phase-sensitive) tone detector using an ultra-selective bandpass filter, such as the LTC1164-8. The ultra-narrow passband of the LTC1164-8 filter band-limits any random noise and increases the detector's signal sensitivity.

The LTC1164-8 is an eighth-order, elliptic bandpass filter, with the following features: the filter's  $f_{\text{CENTER}}$  (the center frequency of the filter's passband) is clock tunable and is equal to the clock frequency divided by 100; the filter's passband is from  $0.995 \times f_{\text{CENTER}}$  to  $1.005 \times f_{\text{CENTER}}$  ( $\pm 0.5\%$  from  $f_{\text{CENTER}}$ ). Figure 1 shows a typical LTC1164-8 passband response and the area of passband-gain variation. Outside the filter's passband, signal attenuation increases to more than 50dB for frequencies between  $0.96 \times f_{\text{CENTER}}$  and  $1.04 \times f_{\text{CENTER}}$ . Quiescent current is typically 2.3mA with a single 5V power supply.

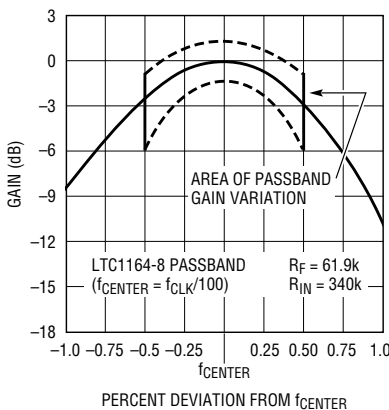


Figure 1. Detail of LTC1164-8 passband

## An Ultra-Selective Bandpass Filter and a Dual Comparator Build a High-Performance Tone Detector

The LTC1164-8 has excellent selectivity, which limits the noise that passes from the input to the output of the filter. As a result, one can build a tone detector that can extract small signals from the "mud." Figure 2 shows the block diagram of such a tone detector. The detector's input is an LTC1164-8 bandpass filter whose output is AC coupled to a dual comparator circuit. The first comparator converts the filter's output to a variable pulsewidth signal. The pulsewidth varies depending on the signal amplitude. The average DC value of the pulse signal is extracted by a lowpass RC filter and applied to the second comparator. The identification of a tone is indicated by a logic high at the output of the second comparator.

One of the key benefits of using a high-selectivity bandpass filter for tone detection is that when wideband noise (white noise) appears at the input of the filter, only a small amount of input noise will reach the filter's output. This results in a dramatically improved signal to noise ratio at the output of the filter compared to the signal-to-noise at the input of the

filter. If the output noise of the LTC1164-8 is neglected, the signal to noise ratio at the output of the filter divided by the signal to noise ratio at the input of the filter is:

$$\frac{(S/N)_{\text{OUT}}}{(S/N)_{\text{IN}}} = 20 \text{ Log } \sqrt{\frac{(BW)_{\text{IN}}}{(BW)_{\text{f}}}}$$

where:  $(BW)_{\text{IN}}$  = the noise bandwidth at the input of the filter and  $(BW)_{\text{f}} = 0.01 \times (f_{\text{CENTER}})$  is the filter's noise equivalent bandwidth.

For example, a small 1kHz signal is sent through a cable that is also conducting random noise with a 3.4kHz bandwidth. An LTC1164-8 is used to detect the 1kHz signal. The signal-to-noise ratio at the output of the filter is 25.3db larger than the signal-to-noise ratio at the input of the filter:

$$\sqrt{\frac{(BW)_{\text{IN}}}{(BW)_{\text{f}}}} = 20 \text{ Log } \sqrt{\frac{3.4\text{kHz}}{0.01 \times 1\text{kHz}}} = 25.3\text{dB}$$

Figure 3 shows the complete circuit for a 1kHz tone detector operating with a single 5V supply. An LTC1164-8 with a clock input set at 100kHz sets the tone detector's frequency at 1kHz ( $f_{\text{CENTER}} = f_{\text{CLK}}/100$ ). A low-frequency op amp (LT1013) and resistors  $R_{\text{IN}}$  and  $R_{\text{F}}$  set the filter's gain. In order to minimize the filter's

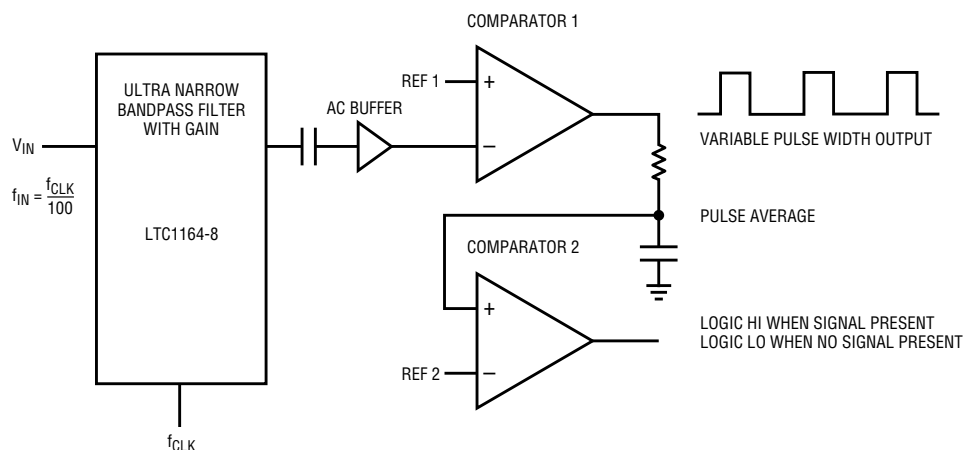


Figure 2. Tone detector block diagram

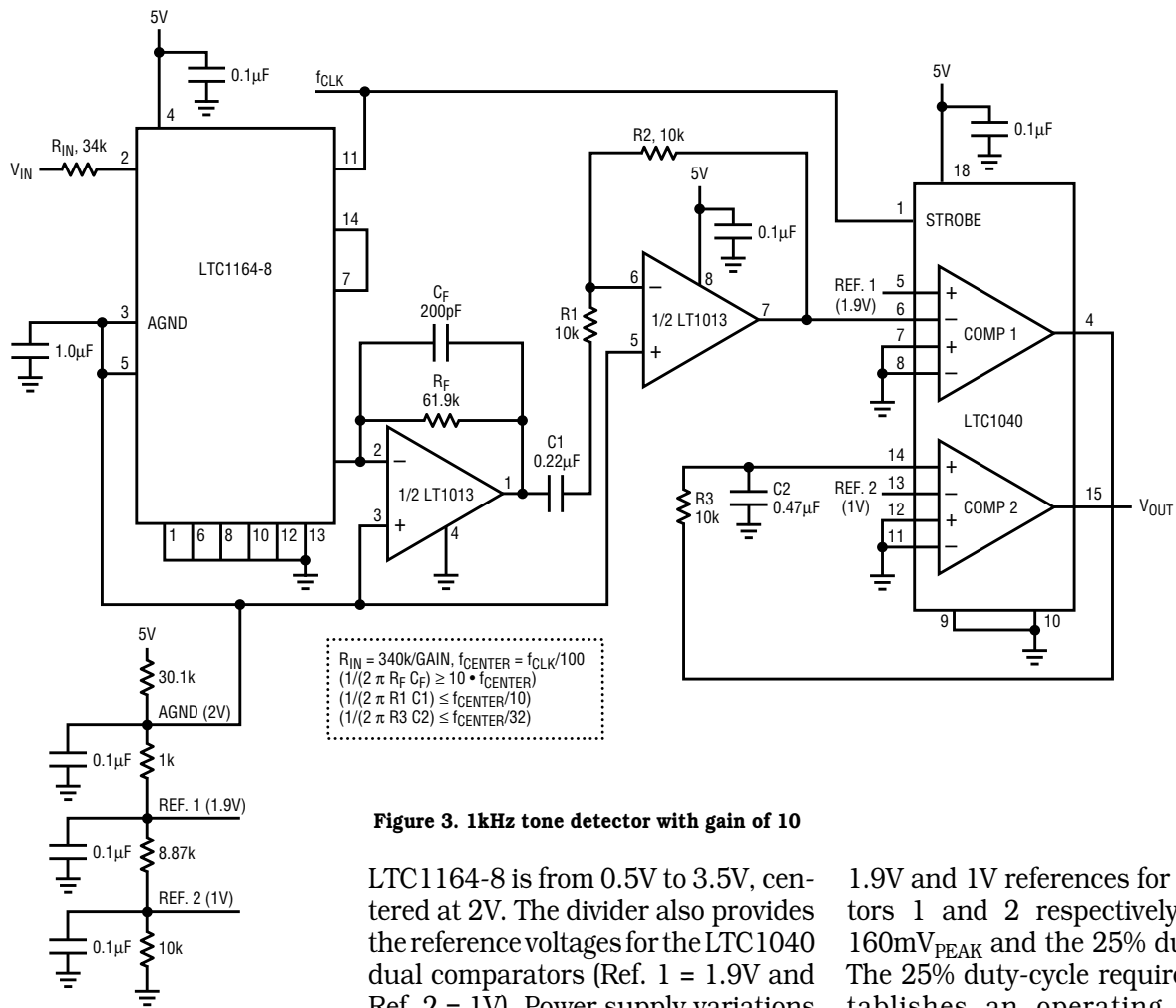


Figure 3. 1kHz tone detector with gain of 10

output noise and maintain optimum dynamic range, the output feedback resistor  $R_F$  should be 61.9k. Capacitor  $C_F$  across resistor  $R_F$  is added to reduce the clock feedthrough at the filter's output.

To set the gain for the LTC1164-8,  $R_{IN}$  should be calculated by the equation:

$$R_{IN} = 340k/\text{gain}$$

In Figure 3, the filter's gain is 10 ( $R_{IN} = 34k$ ). Capacitor  $C_1$  and a unity-gain op amp (LT1013) AC couple the signal at the filter's output to an LTC1040 dual low-power comparator. AC coupling is required to eliminate any DC offset caused by the LTC1164-8.

A resistive divider generates a 2V bias for the LTC1164-8 "ground" (pins 3 and 5) and the positive input of the LT1013 dual op amps. For single 5V operation, the output swing of the

LTC1164-8 is from 0.5V to 3.5V, centered at 2V. The divider also provides the reference voltages for the LTC1040 dual comparators (Ref. 1 = 1.9V and Ref. 2 = 1V). Power supply variations do not affect the performance of this circuit because all DC reference voltages are derived from the same resistor divider and will track any changes in the 5V power supply.

### Theory of Operation

The tone detector works by looking at the negative peaks at the output of the filter. Signals below 1.9V at the output of the filter trip the first comparator. The second comparator has a 1V reference and detects the average value of the output of the first comparator. The R3-C2 time constant is set to allow detection only if the duty cycle of the first comparator's output exceeds 25%. Waveforms with duty cycles below 25% are arbitrarily assumed to carry false information.

The circuitry is designed so that two or more negative signal peaks of 160mV at the filter's output produce a 25% duty-cycle pulse waveform at the output of the first detector (the

1.9V and 1V references for comparators 1 and 2 respectively, set the 160mV<sub>PEAK</sub> and the 25% duty cycle). The 25% duty-cycle requirement establishes an operating point or "minimum detectable signal" for the detector circuit. Thus, the circuitry outputs a "tone-present" condition only when the duty cycle is greater than or equal to 25%. The 25% duty-cycle requirement sets two conditions for optimum tone detection at the detector's input.

The first input condition is the maximum-input-noise spectral density that will not trigger the detector's output to indicate the presence of a tone. When only noise is present at the filter's input, the maximum-input-noise spectral density is conservatively defined as the amount required to produce noise peaks at the filter's output of 160mV or lower amplitude. The 160mV maximum noise-peak specification at the filter's output can be converted to output noise in mV<sub>RMS</sub> by using a crest factor of 5 (the crest factor of a signal is the ratio of its peak value to its RMS value—a theoretical crest factor of 5

predicts 99.3% of the maximum peaks of wideband noise with uniform spectral density). Therefore, the maximum allowable noise at the filter's output is  $32\text{mV}_{\text{RMS}}$  ( $160\text{mV}_{\text{PEAK}}/5$ ). The noise at the filter's output depends on the filter's gain and noise equivalent bandwidth and the spectral density of the noise at the filter's input. Therefore, the maximum input noise spectral density for Figure 3's circuit is:

$$e_{\text{IN}} \leq 32\text{mV}_{\text{RMS}} / (\text{Gain} \times \sqrt{(\text{BW})_f}) \frac{V_{\text{RMS}}}{\sqrt{\text{Hz}}}$$

where: Gain is the filter's gain at its center frequency and  $(\text{BW})_f$  is the filter's noise-equivalent bandwidth.

Note: Compared to  $32\text{mV}_{\text{RMS}}$ , the  $270\mu\text{V}_{\text{RMS}}$  output noise of the LTC1164-8 is negligible. The output

noise of the LTC1164-8 is independent of the chosen filter signal gain.

The second input condition is the minimum input signal required so that a tone can be detected when it is buried by the maximum noise, as defined by the first input condition. When a tone plus noise are present at the filter's input, the output of the filter will be a tone whose amplitude is modulated by the bandlimited noise at the filter's output. If a maximum noise peak of  $160\text{mV}$  modulates the tone's amplitude, a  $320\text{mV}$  tone peak at the filter's output can be detected because the product of the noise and the tone crosses the (negative)  $160\text{mV}_{\text{PEAK}}$  detection threshold and the 25% duty cycle requirement is exceeded. Therefore, a conservative value for the minimum signal at the

filter's output can be set to  $320\text{mV}_{\text{PEAK}}$  or  $226\text{mV}_{\text{RMS}}$ , but a value of  $200\text{mV}_{\text{RMS}}$  was established experimentally. Therefore, the minimum input signal for reliable tone detection in the presence of the maximum input-noise spectral density is:

$$V_{\text{IN}} (\text{MIN.}) = 200\text{mV}_{\text{RMS}} / \text{Gain}$$

For optimum tone detection, the signal's frequency should be in the filter's passband, within  $\pm 0.1\%$  of  $f_{\text{CENTER}}$ .

**Conclusion**

A very selective bandpass filter, the LTC1164-8, can be configured as a non-phase-sensitive tone detector. This allows signals to be detected in the presence of comparatively large amounts of noise or signal-to-noise ratios that are less than unity. **LT**

# High Output-Current Boost Regulator

by Dimitry Goder

Low-voltage switching regulators are often implemented with self-contained power integrated circuits featuring a PWM controller and an onboard power switch. Maximum switching currents of up to 10A are available, providing a convenient means for power conversion over wide input- and output-voltage ranges. However, if higher switching currents are required, a switching regulator controller with an external power MOSFET is a better choice.

Figure 1 shows an LTC1147-based 5V-to-12V converter with 3.5A peak output-current capability. The LTC1147 is a micropower controller that uses a constant off-time architecture, eliminating the need for external slope compensation. Current-mode control allows fast transient response and cycle-by-cycle current limiting. A maximum voltage of only 150 millivolts across the current-sense resistor R7 optimizes performance for low input voltages.

When Q2 turns on, current starts building up in inductor L1. This pro-

vides a ramping voltage across R7. When this voltage reaches a threshold value set internally in the LTC1147, Q2 turns off and the energy stored in L1 is transferred to the output capacitor C5. Timing capacitor C2 sets the operating frequency. The controller is powered from the output through R5, providing 10V of

gate drive for Q2. This reduces the MOSFET's on-resistance and allows efficiency to exceed 90% even at full load. The feedback network comprising R2 and R8 sets the output voltage. Current sense resistor R7 sets the maximum output current; it can be changed to meet different circuit requirements. **LT**

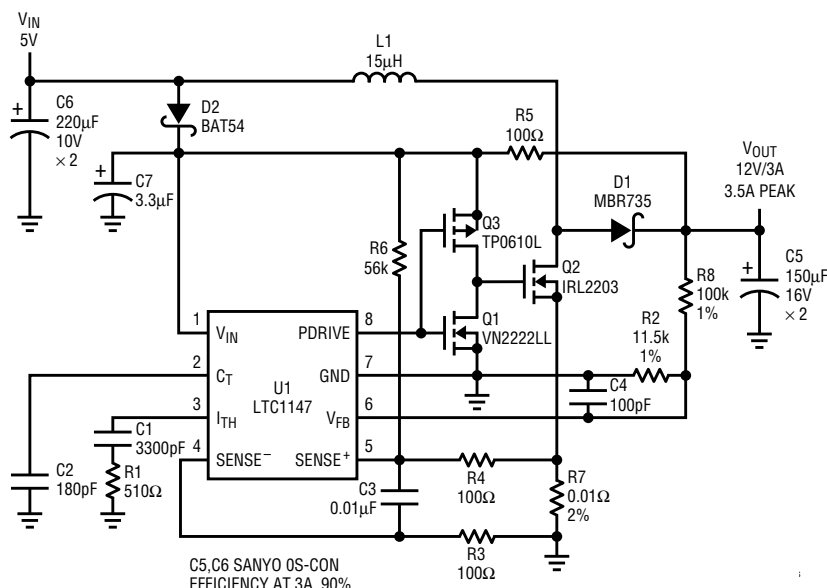


Figure 1. LTC1147-based 5V-to-12V converter



# High-Efficiency EL Driver Circuit

by Dave Bell

Electroluminescent (EL) lamps are gaining popularity as sources of LCD-backlight illumination, especially in small, handheld products. EL lamps resemble thin sheets of cardboard and are available in a variety of colors. Compared with other backlighting technologies, EL is attractive because the lamp is thin, lightweight, rugged, and can be illuminated with little power. Moreover, light is emitted uniformly from the entire EL surface, so no diffuser is needed.

EL lamps are capacitive in nature, typically exhibiting around 3000pF/in<sup>2</sup>, and require a low frequency (50Hz–1kHz) 120V<sub>RMS</sub> AC drive voltage. Heretofore, this has usually been generated by a low-frequency blocking oscillator using a large transformer. These large, inefficient power modules have been suitable for traditional EL applications, such as emergency exit signs and instrument panel backlights, but such space and power inefficiencies are unacceptable in lightweight, battery-powered products.

Figure 1 depicts a high-efficiency EL driver that can drive a relatively large (12 in<sup>2</sup>) EL lamp using a small high-frequency transformer. The circuit is self oscillating, and delivers a regulated triangle wave to the attached lamp. Very high conversion efficiency may be obtained using this circuit, even matching state-of-the-art CCFL backlights at modest brightness levels (10–20 foot-lamberts).

Since an EL lamp is basically a lossy capacitor, the majority of the energy delivered to the lamp during the charge half-cycle is stored as electrostatic energy ( $1/2CV^2$ ). Overall conversion efficiency can be improved by almost 2:1 if this stored energy is returned to the battery during the discharge half-cycle. The circuit of Figure 1 operates as a flyback converter during the charge half-cycle, taking energy from the battery and charging the EL capacitance. During

the discharge half-cycle, the flyback converter operates in the reverse direction, taking energy back out of the EL lamp and returning it to the battery. Nearly 50% of the energy taken during the charge half-cycle is returned during the discharge half-cycle; hence the 2:1 efficiency improvement.

During the charge half-cycle, the LT1303 operates as a flyback converter at approximately 150kHz, ramping the current in T1's 10μH primary inductance to approximately 1A on each switching pulse. When the LT1303's internal power switch turns off, the flyback energy stored in T1 is delivered to the EL lamp through D3 and C5. Successive high-frequency flyback cycles progressively charge the EL capacitance until 300V is reached on the "+" side of C5. At this point, the feedback voltage present at the LT1303's LBI input reaches 1.25V, causing the internal comparator to change state.

When the LT1303's internal comparator changes state, the open-collector driver at the LBO output is released. This places the circuit into discharge mode, and reverses the operation of the flyback energy transfer. Q3 turns on, removing the gate drive from Q2A, thereby disabling switching action on the primary of T1. Flip-flop U2A is also clocked, resulting in a high level on the Q-bar output; this positive feedback action keeps LBI above 1.25V. Even though Q2A is turned off, the LT1303's SW pin still switches into pull-up resistor R4. The resulting pulses at the SW pin are used to clock U2B and to drive a "poor man's" current-mode flyback converter on the secondary of T1.

Every clock pulse to flip-flop U2B turns on Q2B and draws current from the EL lamp through C5, T1, D2, and Q4. (Q4 must be a 600V-rated MOSFET to withstand the high peak voltages present on its drain during normal operation.) Current ramps

up through T1's 2.25mH secondary inductance until the voltage across current-sense resistor R12 reaches approximately 0.6V. At this point Q5 turns on, providing a direct clear to U2B and thereby terminating the pulse. Energy taken from the EL lamp and stored in T1's inductance is then transferred back to the battery through D1 and T1's primary winding. This cycle repeats at approximately 150kHz until the voltage on C5 ratchets down to approximately zero volts. Once C5 is fully discharged, the pre-set input on U2A will be pulled low, forcing the voltage on the LT1303's LBI input to ground, and initiating another charge half-cycle.

This circuit produces a triangle voltage waveform with a constant peak-to-peak voltage of 300V, but the frequency of the triangle wave depends on the capacitance of the attached EL lamp. A 12 in<sup>2</sup> lamp has approximately 36nF of capacitance, which results in a triangle wave frequency of approximately 400Hz. This produces approximately 17FL of light output from a state-of-the-art EL lamp. Because of the "constant power" nature of the charging flyback converter, light output remains relatively constant with changes in the battery voltage. In addition, since EL lamp capacitance decreases with age, the circuit tends to minimize brightness reduction with lamp aging. C5, R9, and R10 maintain a zero average voltage across the EL lamp terminals—an essential factor for reliable lamp operation.

Two options exist for EL lamps with different characteristics. Larger lamps can be supported by specifying an LT1305 instead of the LT1303 shown in Figure 1. The LT1305 will terminate switch cycles at 2A instead of 1A, thereby delivering four times as much energy (energy stored in T1 is defined by  $1/2LI^2$ ). The value of R12 must also be reduced to 7.5Ω to increase the discharge flyback current by the same ratio. For smaller



# Adding Features to the Boost Topology

by Dimitry Goder

A boost-topology switching regulator is the simplest solution for converting a two- or three-cell input to a 5V output. Unfortunately, boost regulators have some inherent disadvantages, including no short-circuit protection and no shutdown capability. In some battery-operated products, external chargers or adapters can raise the battery voltage to a potential higher than the 5V output. Under this condition, a boost converter cannot maintain regulation—the high input voltage feeds through the diode to the output.

The circuit shown in Figure 1 overcomes these problems. An LT1301 is used as a conventional boost converter, preserving simplicity and high efficiency in the boost mode. Transistor Q1 adds short-circuit limiting, true shutdown, and regulation when there is a high input voltage.

When the input voltage is lower than 4V and the regulator is enabled, Q1's emitter is driven above its base, saturating the transistor. As a result, the voltages on C1 and C2 are roughly the same, and the circuit operates as a conventional boost regulator.

If the input voltage increases above 4V, the internal error amplifier, acting to keep the output at 5V, boosts the voltage on C1 to a level greater than 1V above the input. This voltage controls Q1 to provide the desired output, with the transistor operating as a linear pass element. The output does not change abruptly during the switch-over between step-up and step-down modes, because it is monitored in both modes by the same error amplifier.

Figure 2 shows efficiency versus input voltage for 5V/100mA output. The break point at 4.25V is evidence of Q1 beginning to operate in a linear

mode, with an attendant roll-off of efficiency. Below 4.25V the circuit operates as a boost regulator, and maintains high efficiency across a broad range of input voltages.

The circuit can be shut down by pulling the LT1301's shutdown pin high. The LT1301 ceases switching and Q1 automatically turns off, fully disconnecting the output. This stays true over the entire input voltage range.

Q1 also provides overload protection. When the output is shorted, the LT1301 operates in a cycle-by-cycle current limit. The short-circuit current depends on the maximum switch current of the LT1301 and on the Q1's gain, typically reaching 200mA. The transistor can withstand overload for several seconds, before heating up. For sustained faults, the thermal effects on Q1 should be carefully considered. 

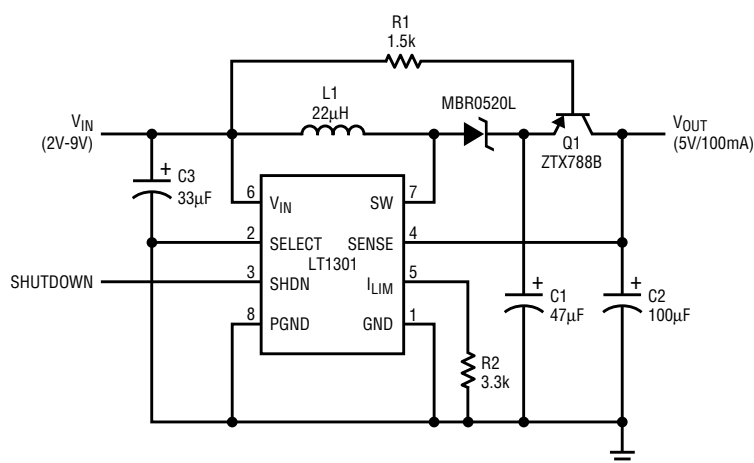


Figure 1. Q1 adds short-circuit limiting, true shutdown and regulation when there is a high input voltage to the LT1301 in boost mode

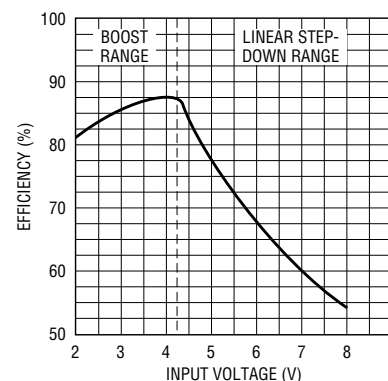


Figure 2. Efficiency versus input for voltages for 5V/100mA output

# Bandpass Filter Has Adjustable Q

by Frank Cox

The bandpass-filter circuit shown in Figure 1 features an electronically controlled Q. Q for a bandpass filter is defined as the ratio of the 3dB pass bandwidth to the stop bandwidth at some specified attenuation. The center frequency of the bandpass filter in this example is 3MHz, but this can be adjusted with appropriate LC-tank components. The upper limit of the usable frequency range is about 10MHz. The width of the passband is adjusted by the current into pin 5 (set current or  $I_{SET}$ ) of the transconductance amplifier segment of IC1, an LT1228. Figure 2 (page 33) is a network-analyzer plot of frequency response verses set current. This plot shows the variation in Q while the center frequency and the passband gain remain relatively constant.

The circuit's operation is best understood by analyzing the closed-loop transfer function. This can be written in the form of the classic negative-feedback equation:

$$H(s) = \frac{A(s)}{1 + A(s) B(s)}$$

where A(s) is the forward gain and B(s) is the reverse gain. The forward gain is the product of the transconductance stage gain ( $g_m$ ) and the gain of the CFA ( $A_{CFA}$ ). For this circuit,  $g_m$  is ten times the product of  $I_{SET}$  and the impedance of the tank circuit as a function of frequency. This gives the

complete expression for the forward gain as a function of frequency:

$$A(s) = 10 I_{SET} A_{CFA} \left( \frac{sL}{1 + s^2 LC} \right)$$

The reverse gain is simply:

$$B(s) = \frac{R7}{R6 + R7}$$

$$\text{and } A_{CFA} = \frac{R4 + R5}{R4}$$

$$\text{Setting } B(s) = \frac{1}{A_{CFA}} = R_{RATIO}$$

and substituting these expressions into the first equation gives:

$$H(s) = \frac{1}{R_{RATIO}} \frac{10 I_{SET} \left( \frac{sL}{1 + s^2 LC} \right)}{1 + 10 I_{SET} \left( \frac{sL}{1 + s^2 LC} \right)}$$

The last equation can be rewritten as:

$$H(s) = \frac{1}{R_{RATIO}} \frac{S \left[ \frac{1}{\sqrt{LC}} \left( \frac{10 I_{SET} \sqrt{LC}}{C} \right) \right]}{S^2 + S \left[ \frac{1}{\sqrt{LC}} \left( \frac{10 I_{SET} \sqrt{LC}}{C} \right) \right] + \frac{1}{\sqrt{LC}}}$$

The transfer function of a second order bandpass filter can be expressed in the form<sup>1</sup>:

$$H(s) = H_{BP} \frac{S(\omega_o/Q)}{S^2 + S(\omega_o/Q) + \omega_o^2}$$

Comparing the last two equations note that

$$\omega_o = \frac{1}{\sqrt{LC}} \quad \text{and} \quad \frac{1}{Q} = \frac{10 I_{SET} \sqrt{LC}}{C}$$

$$\text{And therefore } Q = \frac{C}{10 I_{SET} \sqrt{LC}}$$

It can be seen from the last equation that the Q is inversely proportional to the set current.

Many variations of the circuit are possible. The center frequency of the filter can be tuned over a small range by the addition of a varactor diode. To increase the maximum realizable Q, add a series LC network tuned to the same frequency as the LC tank on pin 1 of IC1. To lower the minimum obtainable Q, add a resistor in parallel with the tank circuit. To create a variable-Q notch filter, connect the inductor and capacitor at pin 1 in series rather than in parallel.

A variable-Q bandpass filter can be used to make a variable-bandwidth IF or RF stage. Another application for this circuit is as a variable-loop filter in a phase-lock-loop phase demodulator. The variable-Q bandpass filter is set for a wide bandwidth while the loop acquires the signal and is then adjusted to a narrow bandwidth for best noise performance after lock is achieved.

1. Thanks to Doug La Porte for this equation hack.

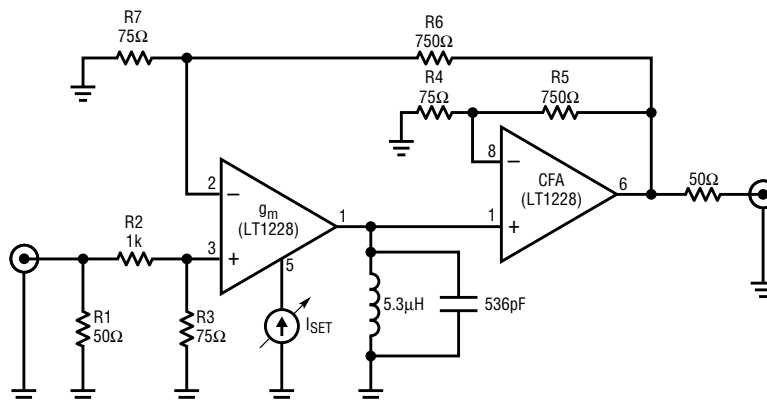


Figure 1. Circuit diagram: LT1228 bandpass filter

# Sallen and Key Filters Use 5% Values

by Dale Eagar

Lowpass filters designed after Sallen and Key usually take the form shown in Figure 1. In the classic Sallen and Key circuit, resistors R1, R2, and R3 are set to the same value to simplify the design equations.

When the three resistors are the same value, the pole placement, and thus the filter characteristics, are set by the capacitor values (C1, C2, and

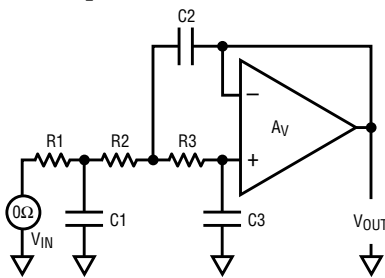


Figure 1. Sallen and Key lowpass filter

C3). This procedure, although great for the mathematician, can lead to problems. The problem is that, in the real world, the resistors, not the capacitors, are available in a large selection of values.

Taking advantage of the wider range of resistor values is not altogether trivial; the mathematics can be quite cumbersome and time consuming.

This Design Idea includes tables of resistor and capacitor values for third-order Sallen and Key lowpass filters. The resistor values are selected from the standard 5% value pool, and the capacitor values are selected from the standard 10% value pool. Frequencies are selected from the standard 5% value pool used for resistors. Frequencies are in Hertz, capacitance in Farads, and resistance in Ohms.

Figure 2 details the PSpice™ simulation of a 1.6kHz Butterworth filter designed from these tables.

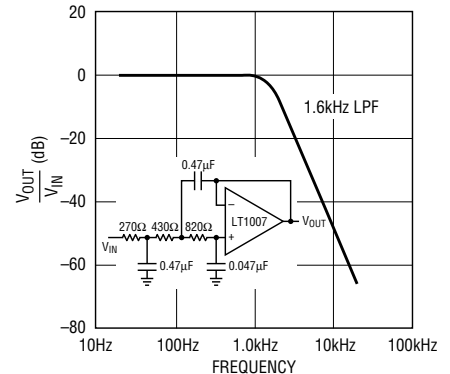


Figure 2. PSpice simulation of 1.6kHz Butterworth filter

Table 1. Bessel lowpass filter

| Freq. | R1   | R2    | R3    | C1   | C2    | C3    |
|-------|------|-------|-------|------|-------|-------|
| 1.0   | 0.39 | 0.43  | 8.20  | 0.47 | 0.22  | 0.01  |
| 1.1   | 0.36 | 0.39  | 7.50  | 0.47 | 0.22  | 0.01  |
| 1.2   | 0.33 | 0.36  | 6.80  | 0.47 | 0.22  | 0.01  |
| 1.3   | 0.36 | 2.40  | 0.033 | 0.22 | 2.20  | 0.047 |
| 1.5   | 0.33 | 4.70  | 0.012 | 0.22 | 4.70  | 0.022 |
| 1.6   | 0.30 | 0.10  | 0.240 | 0.47 | 2.20  | 0.047 |
| 1.8   | 0.30 | 3.30  | 5.10  | 0.22 | 0.022 | 0.010 |
| 2.0   | 0.27 | 0.51  | 0.027 | 0.22 | 2.20  | 0.100 |
| 2.2   | 0.24 | 2.70  | 0.43  | 0.22 | 0.10  | 0.022 |
| 2.4   | 0.22 | 2.70  | 3.60  | 0.22 | 0.022 | 0.010 |
| 2.7   | 0.27 | 0.43  | 1.30  | 0.22 | 0.10  | 0.022 |
| 3.0   | 0.18 | 0.82  | 0.16  | 0.22 | 0.22  | 0.047 |
| 3.3   | 0.15 | 0.056 | 1.00  | 0.47 | 1.00  | 0.010 |
| 3.6   | 0.18 | 0.16  | 0.022 | 0.22 | 2.20  | 0.100 |
| 3.9   | 0.15 | 1.50  | 2.20  | 0.22 | 0.022 | 0.010 |
| 4.3   | 0.13 | 0.22  | 0.013 | 0.22 | 2.20  | 0.100 |
| 4.7   | 0.20 | 0.12  | 1.20  | 0.22 | 0.22  | 0.010 |
| 5.1   | 0.18 | 0.068 | 0.039 | 0.22 | 2.20  | 0.047 |
| 5.6   | 0.20 | 1.10  | 0.036 | 0.10 | 0.47  | 0.022 |
| 6.2   | 0.15 | 0.091 | 0.91  | 0.22 | 0.22  | 0.010 |
| 6.8   | 0.16 | 0.91  | 0.03  | 0.10 | 0.47  | 0.022 |
| 7.5   | 0.15 | 1.80  | 0.27  | 0.10 | 0.047 | 0.010 |
| 8.2   | 0.10 | 0.12  | 1.00  | 0.22 | 0.10  | 0.010 |
| 9.1   | 0.13 | 0.56  | 0.12  | 0.10 | 0.10  | 0.022 |

Table 2. Butterworth lowpass filter

| Freq. | R1   | R2   | R3    | C1   | C2   | C3    |
|-------|------|------|-------|------|------|-------|
| 1.0   | 0.36 | 3.3  | 3.3   | 0.47 | 0.10 | 0.022 |
| 1.1   | 0.47 | 0.47 | 6.2   | 0.47 | 0.47 | 0.010 |
| 1.2   | 0.36 | 0.62 | 1.0   | 0.47 | 0.47 | 0.047 |
| 1.3   | 0.27 | 2.00 | 0.33  | 0.47 | 0.47 | 0.047 |
| 1.5   | 0.24 | 1.60 | 0.3   | 0.47 | 0.47 | 0.047 |
| 1.6   | 0.27 | 0.43 | 0.82  | 0.47 | 0.47 | 0.047 |
| 1.8   | 0.43 | 1.20 | 0.13  | 0.22 | 1.00 | 0.047 |
| 2.0   | 0.36 | 7.50 | 0.18  | 0.22 | 0.47 | 0.010 |
| 2.2   | 0.24 | 0.24 | 3.00  | 0.47 | 0.47 | 0.010 |
| 2.4   | 0.33 | 0.91 | 0.043 | 0.22 | 2.20 | 0.047 |
| 2.7   | 0.27 | 5.60 | 0.062 | 0.22 | 1.00 | 0.010 |
| 3.0   | 0.24 | 5.10 | 0.056 | 0.22 | 1.00 | 0.010 |
| 3.3   | 0.22 | 1.60 | 0.30  | 0.22 | 0.22 | 0.022 |
| 3.6   | 0.22 | 0.56 | 0.068 | 0.22 | 1.00 | 0.047 |
| 3.9   | 0.24 | 0.39 | 0.68  | 0.22 | 0.22 | 0.022 |
| 4.3   | 0.18 | 0.51 | 0.024 | 0.22 | 2.20 | 0.047 |
| 4.7   | 0.16 | 1.30 | 0.039 | 0.22 | 1.00 | 0.022 |
| 5.1   | 0.16 | 0.36 | 0.051 | 0.22 | 1.00 | 0.047 |
| 5.6   | 0.13 | 1.10 | 0.033 | 0.22 | 1.00 | 0.022 |
| 6.2   | 0.13 | 0.36 | 0.016 | 0.22 | 2.20 | 0.047 |
| 6.8   | 0.24 | 1.60 | 0.33  | 0.10 | 0.10 | 0.010 |
| 7.5   | 0.12 | 0.30 | 1.20  | 0.22 | 0.10 | 0.010 |
| 8.2   | 0.12 | 0.11 | 0.024 | 0.22 | 2.20 | 0.047 |
| 9.1   | 0.18 | 1.50 | 0.091 | 0.10 | 0.22 | 0.010 |

### How to Design a Filter from the Tables:

- ❑ Pick a cutoff frequency in Hertz as if it were a standard 5% resistor value in Ohms. (that is, if you want a cutoff frequency of 1.7kHz, you must choose between 1.6k and 1.8k)
- ❑ Select the component values from Table 1 or Table 2 as listed for the frequency (think of the

first two color bands on a resistor).

- ❑ Select a scale factor for the resistors and capacitors from Table 3 by the following method:
  1. Select a diagonal that represents the frequency multiplier (think of the third color band on a 5% resistor).
  2. Choose a particular diagonal box by either choosing a capacitor

multiplier from the rows of the table that give you a desired capacitor value or by choosing a resistor multiplier from the columns of the table that gives you a desired resistance value.

- ❑ Multiply the resistors and capacitors by the scale factors for the rows and columns that intersect at the chosen frequency multiplier box. (for example,  $0.68 \times 1\mu\text{F} = .68\mu\text{F}$ ,  $0.47 \times 1\text{k}\Omega = 470\Omega$ ). 

| Table 3. Frequency multipliers |      |      |      |      |       |       |       |       |       |       |
|--------------------------------|------|------|------|------|-------|-------|-------|-------|-------|-------|
|                                | 0.1Ω | 1Ω   | 10Ω  | 100Ω | 1kΩ   | 10kΩ  | 100kΩ | 1MΩ   | 10MΩ  | 100MΩ |
| 1.0F                           | 10   | 1.0  | 0.1  | 0.01 | 0.001 |       |       |       |       |       |
| 0.1F                           | 100  | 10   | 1.0  | 0.1  | 0.01  | 0.001 |       |       |       |       |
| 10,000μF                       | 1k   | 100  | 10   | 1.0  | 0.1   | 0.01  | 0.001 |       |       |       |
| 1,000μF                        | 10k  | 1k   | 100  | 10   | 1.0   | 0.1   | 0.01  | 0.001 |       |       |
| 100μF                          | 100k | 10k  | 1k   | 100  | 10    | 1.0   | 0.1   | 0.01  | 0.001 |       |
| 10μF                           | 1M   | 100k | 10k  | 1k   | 100   | 10    | 1.0   | 0.1   | 0.01  | 0.001 |
| 1μF                            | 10M  | 1M   | 100k | 10k  | 1k    | 100   | 10    | 1.0   | 0.1   | 0.01  |
| 0.1μF                          | 100M | 10M  | 1M   | 100k | 10k   | 1k    | 100   | 10    | 1.0   | 0.1   |
| 0.01μF                         | 1G   | 100M | 10M  | 1M   | 100k  | 10k   | 1k    | 100   | 10    | 1.0   |
| 1,000pF                        |      | 1G   | 100M | 10M  | 1M    | 100k  | 10k   | 1k    | 100   | 10    |
| 100pF                          |      |      | 1G   | 100M | 10M   | 1M    | 100k  | 10k   | 1k    | 100   |

Bandpass Filter, continued from page 31

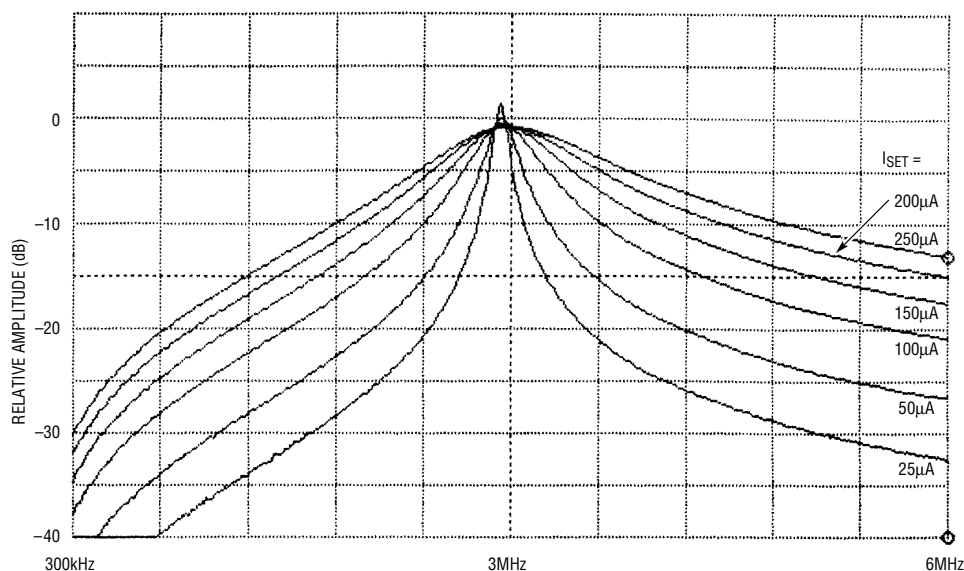


Figure 2. Network-analyzer plot of frequency response verses "set" current

# Simple Battery Charger Runs at 1MHz

by Mitchell Lee

Fast switching regulators have reduced coil sizes to the point that they are no longer the largest components on the board. A case in point is the LT1377, which can operate at 1MHz with inductances under 10 $\mu$ H.

The circuit shown in Figure 1 was designed for a customer who wanted to charge a four-cell NiCd pack from a 5V logic supply. (This circuit will work equally well with a 3.3V input.) Clearly the circuit needs an output voltage greater than 5V, which is handled easily by the LT1377 boost regulator. The output current is limited to approximately 50mA by a  $V_{BE}$  current-sensor (Q1/R1) controlling the feedback pin (2) of the LT1377. This current is perfect for slow charging or trickle charging AA NiCd batteries.

Battery chargers are commonly subject to a number of fault conditions, which must be addressed in the design phase. First, what hap-

pens when the battery is disconnected? In a boost regulator, the output voltage will increase without bound and blow up either the output capacitor or switch. Some voltage limiting is necessary, and in this design D2 serves the purpose. If the voltage on C3 rises to 11.25V, D2 takes over the control loop at the feedback pin.

Another potential calamity is an output short circuit; a related fault results from connecting a battery pack containing one or more shorted cells, such that the terminal voltage is less than about 4V. Under either of these circumstances, unlimited current flows from the 5V input supply, through D1 and Q1's base-emitter junction, frying at least Q1.

Q2 has been added to allow full current control even when the output voltage is less than the input voltage. In normal operation, where the output is boosted higher than 5V, Q2 is fully on. Its gate is held at 1.25V (pin

2 feedback voltage), and its source is greater than 5V; hence it has no choice but to be fully enhanced. Q2 becomes more functional when the output voltage drops to around 4V. First of all, at 4V input the switching regulator stops switching because more than 50mA current flows and the feedback pin is pulled up above 1.25V—Q1 makes sure of that. But as Q1's collector continues to rise, Q2 is gradually cut off, at least to the extent necessary to starve the drain current back to about 50mA. This action works right down to  $V_{OUT} = 0$ . In a short-circuit, Q2 dissipates about 200mW, not too much for a surface-mount MOSFET.

This circuit is useful for four to six cells, and the output current can be modified somewhat by changing sense resistor R1. A reasonable range is from very low currents (1mA or less) up to 100mA. The current will diminish as Q1's  $V_{BE}$  drops about 0.3%/°C with temperature.  $\blacktriangleleft$

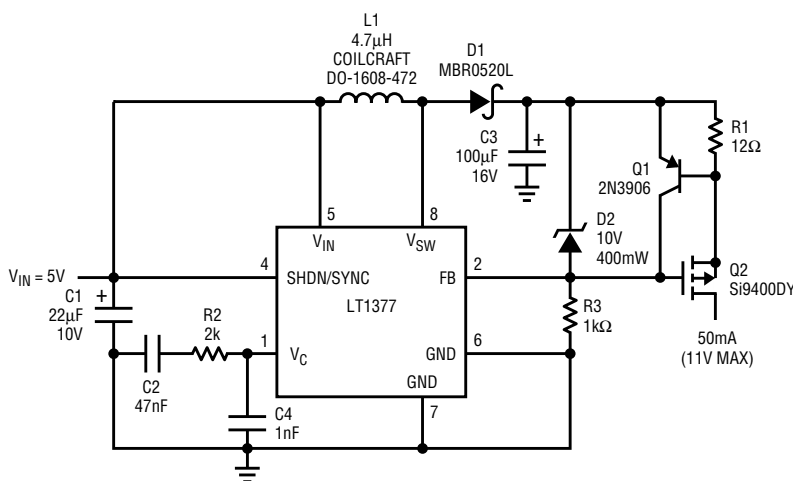


Figure 1. Battery charger schematic diagram

# Lithium-Ion Battery Charger

by Dimitry Goder

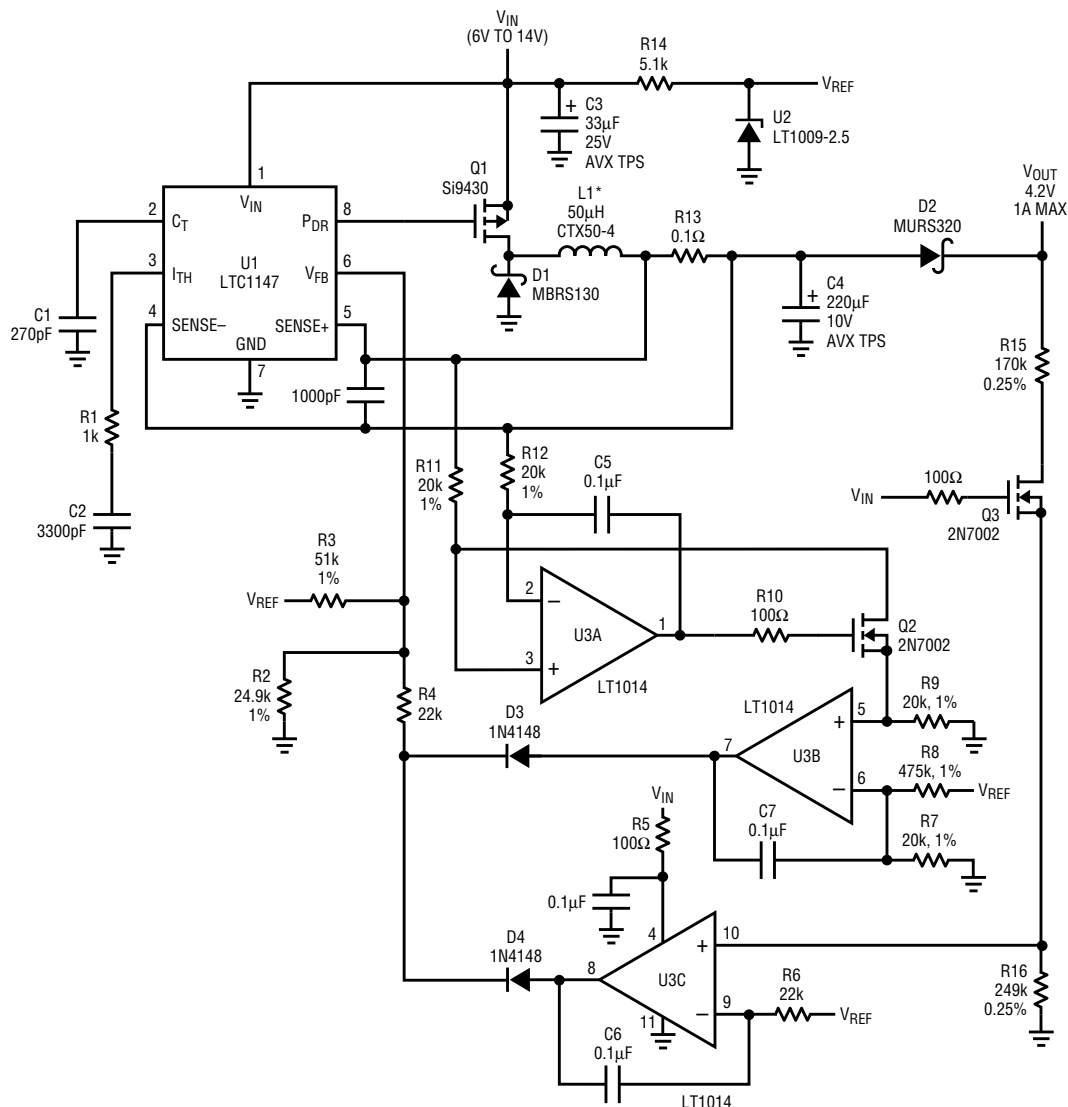
Lithium-ion (Li-Ion) rechargeable batteries are quickly gaining popularity in a variety of applications. The main reasons for the success of Li-Ion cells are higher power density and higher terminal voltage compared to other currently available battery technologies. The basic charging principle for a Li-Ion battery is quite simple: apply a constant voltage source with a built-in current limit. A depleted battery is charged with a constant current until it reaches a specific voltage (usually 4.2V per cell),

then it floats at this voltage for an indefinite period. The main difficulty with charging Li-Ion cells is that the floating-voltage accuracy needs to be around 1%, with 5% current-limit accuracy. These two targets are fairly difficult to achieve. Figure 1 shows the schematic of a full solution for a Li-Ion charger.

The battery charger is built around the LTC1147, a high-efficiency step-down regulator controller. The IC's constant off-time architecture and current-mode control ensure circuit

simplicity and fast transient response. At the beginning of the on-cycle, P-channel MOSFET Q1 turns on and the current ramps up in the inductor. An internal current comparator senses the voltage, proportional to the inductor current, across sense resistor R13. When this voltage reaches a preset value, the LTC1147 turns Q1 off for a fixed period of time set by C1. After the off-time, the cycle repeats.

To provide an accurate current limit, U3A and Q2 are used to sense



\*L1 = CTX50-4  
COILTRONICS (407) 241-7876

Figure 1. Li-Ion battery charger schematic

the charging current separately from the LTC1147. U3A forces the voltage across R11 to match the average drop across the current sense resistor R13. This voltage sets Q2's drain current, which flows unchanged to the source. As a result, the same voltage appears across R9, which is now referenced to ground. Since C5 provides high-frequency filtering, U3A shifts the average value of the output current. N-channel MOSFET Q2 ensures correct circuit operation even under short-circuit conditions by allowing current sensing at potentials close to ground.

U3B monitors voltage across R9 and acts to keep it constant by comparing it to the reference voltage. Diode D3 is connected in series with U3B's output, allowing the circuit to operate as a current limiter. The current-feedback circuit is not active if the output current limit has not been reached.

U3C provides the voltage feedback by comparing the output voltage to the reference. The feedback resistor ratio ( $R16/(R15 + R16)$ ) sets the output at exactly 4.2V. U3C has a diode (D4) connected in series with its output. This diode ensures that the

voltage- and current-feedback circuits do not operate at the same time. The reference voltage is supplied by the LT1009, with a guaranteed initial tolerance of 0.2%. Together with the 0.25% feedback resistors, the circuit provides less than 1% output-voltage error over temperature.

When the input voltage is not present, Q3 is automatically turned off and the feedback resistors do not discharge the battery. Diode D2 is connected in series with the output, preventing the battery from supplying reverse current to the charger.

# Three-Cell to 3.3V Buck-Boost Converter

by Dimitry Goder

Obtaining 3.3V from three 1.2V (nominal) cells is not a straightforward task. Since battery voltage can be either below or above the output, common step-up or step-down converters are inadequate. Alternatives include using more complex switching topologies, such as SEPIC, or a switching boost regulator plus a series, linear-pass element. Figure 1 presents an elegant implementation of the latter approach.

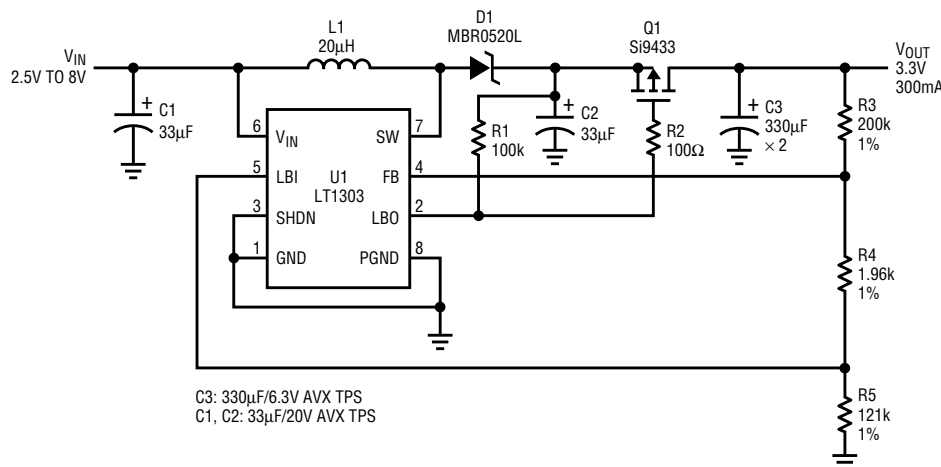
The LT1303 is a Burst Mode™ switching regulator that contains control circuitry, an onboard power

transistor, and a gain block. When the input voltage is below the output, U1 starts switching and boosts the voltage across C2 and C3 to 3.3V. The gain block turns on Q1, because the feedback network R3-R5 biases the low-battery comparator input (LBI) 20mV below the reference. In this mode the circuit operates as a conventional boost converter, sensing output voltage at the FB pin.

When the input voltage increases, it eventually reaches a point where the regulator ceases switching and the input voltage is passed unchanged

to capacitor C2. The output voltage rises until the LBI input reaches the reference voltage of 1.25V, at which point Q1 starts operating as a series-pass element. In these conditions, the circuit functions as a linear regulator, with the attending efficiency roll-off at higher input voltages.

For input voltages derived from three NiCd or NiMH cells, the circuit described provides excellent efficiency and the longest battery life. At 3.6V, where the battery spends most of its life, efficiency exceeds 91%, leaving all alternative topologies far behind.



C3: 330µF/6.3V AVX TPS  
C1, C2: 33µF/20V AVX TPS

Figure 1. Three-cell to 3.3V buck-boost converter

# High Output-Voltage Buck Regulator

by Dimitry Goder

High-efficiency step-down conversion is easy to implement using the LTC1149 as a buck switching-regulator controller. The LTC1149 features constant off-time, current-mode architecture and fully synchronous rectification. Current-mode operation was selected for its well known advantages of clean start-up, accurate current limit, and excellent transient response.

Inductor current sensing is usually implemented by placing a resistor in series with the coil, but the com-

mon-mode voltage at the LTC1149's sense pins is limited to 10V. If a higher output voltage is required, the current-sense resistor can be placed in the circuit's ground return to avoid common-mode problems. The circuit in Figure 1 can be used in applications that do not lend themselves to this approach.

Figure 1 shows a special level-shifting circuit (Q1 and U2) added to a typical LTC1149 application. The LT1211, a high-speed precision amplifier, forces the voltage across R5 to

equal the voltage across current-sense resistor R8. Q1's drain current flows to the source, creating a voltage across R6 proportional to the inductor current, which is now referenced to ground. This voltage can be directly applied to the current-sense inputs of U1, the LTC1149. C12 and C4 are added to improve high-frequency noise immunity. Maximum input voltage is now limited by the LT1211; it can be increased if a zener diode is placed in parallel with C12. 

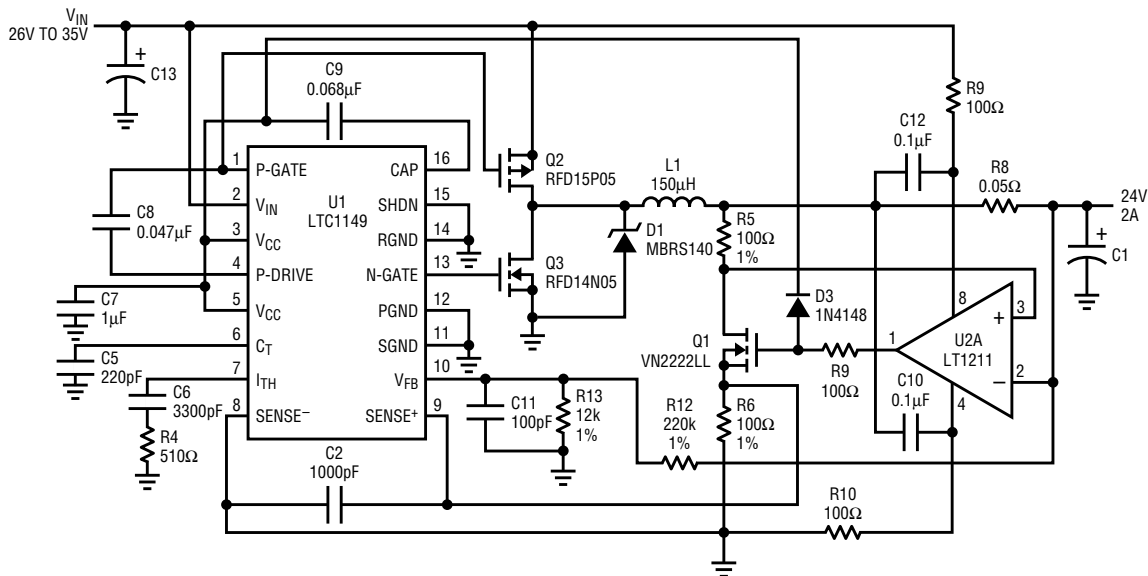


Figure 1. High output-voltage buck regulator schematic using LTC1149

# New Device Cameos

## **LT1239: Backup Battery Management Circuit**

The LT1239 is a micropower device designed to be a complete management system for backup batteries in portable computers and other portable devices. The device can provide both charging and regulating functions for either lithium-ion or NiCd backup batteries. The LT1239 provides an uninterruptable power source for the system's backup memory and power-management circuitry. All circuitry is designed to run at micropower quiescent-current levels.

An adjustable linear regulator supplies a current-limited constant-voltage charge to the backup batteries. This regulator, normally powered from the system's main battery pack, has a quiescent current of 15 $\mu$ A and extremely low reverse-output current. The regulator acts like a switch, charging the backup cells when the main battery pack is connected and disconnecting the backup cells from the charging circuitry when the main batteries are disconnected or discharged. The output voltage is adjustable from 3.75V to 20V. Because of safety considerations related to the use of lithium-ion backup batteries, the regulator can operate with external current-limiting resistors in series with its output. These current-limiting resistors can be placed in the feedback loop of the regulator so that they will not affect output voltage regulation for normal operating conditions.

A second low-dropout linear regulator with a fixed output voltage of 4.85V regulates the output of the backup batteries. This second regulator also acts as a switch. When the system's main battery is providing power, the output of this regulator is pulled up to 5V and no power is drained from the backup cells. If the output of the main power supply drops below 4.85V, the second regulator automatically supplies power from

the backup cells to the backup memory.

The LT1239 contains an error amplifier to equalize the cell voltages in two-cell lithium-ion systems. In addition, it includes a comparator for connecting the main 5V system supply to the backup circuitry.

A low-battery-detector circuit limits the discharge voltage of the backup batteries to 5V. This circuit powers down the 4.85V regulator and error amplifier when the battery voltage drops below 5V. In this shutdown mode the quiescent current drops to 3 $\mu$ A.

Other features include independent shutdown pins for both regulators, and a current-monitor pin for each regulator. The current monitor can be used for gas gauging.

The LT1239 provides all the features needed to build a backup battery management system. The LT1239 is available in a 16-pin, narrow-body SO package.

## **LTC1334 Single 5V RS232/RS485 Transceiver**

The LTC1334 is a single 5V supply, logic configurable, combination RS232 and RS485 transceiver. This new part is targeted at the software-configurable I/O port market.

Combining familiar functions in unfamiliar ways, the LTC1334 offers multiple RS232 and RS485 ports in one package, along with the logic to allow various combinations of port configuration and an onboard charge pump to generate boosted voltages for RS232 levels. Inputs and outputs of both types are packaged together with logic inputs that select which will be active for a given configuration. The LTC1334 features quad RS232 ports and dual RS485 ports, and is configurable as four RS232 transceivers, two RS232 transceivers, and one RS485 transceiver, or two RS485 transceivers. The configu-

ration of these transceivers is set by both PC-trace routing and Select input logic states. For easy multiplexing, all drivers go into a high-impedance state when deselected.

The LTC1334 features micropower shutdown mode, loopback mode for self-test, LTC's usual high data rates (120kbaud for RS232 and 10Mbaud for RS485) and 10kV ESD protection at the driver outputs and receiver inputs.

The LTC1334 is ideal for computers, multiplexers, networks, or peripherals that need to adapt to various I/O configuration requirements without any hardware adjustments. Remember the days of prying off the back cover and throwing DIP switches when you set up your printer? Imagine the problems for a guy with a 90-channel digital MUX—solved by the LTC1334.

The LTC1334 is available in 24 pin SOIC packages.

## **LT1521: Micropower, Low-Dropout Regulator Has 300mA Output-Current Rating**

The LT1521 is a 300mA, low-dropout regulator with a quiescent current of 10 $\mu$ A. Dropout voltage is 150mV at 10mA, rising to 350mV at 300mA. Quiescent current is well controlled in dropout mode; it does not increase significantly as the device enters its dropout region. The device can operate with output capacitors as small as 1 $\mu$ F.

The LT1521 has both reverse-battery and reverse-output protection. Reverse output current is only 6 $\mu$ A, making this device ideal for backup power applications. The LT1521 includes a shutdown feature—quiescent current drops to just 6 $\mu$ A in shutdown conditions. The LT1521 is available in fixed output voltages of 3.0V, 3.3V, and 5.0V. It is also available as an adjustable device with an output-voltage range of 3.75V to 20V. The LT1521 is available in two surface-mount packages: the three-lead SOT-223 and the 8-lead fused-leadframe SO-8.

**LT1528: 3-Amp PNP-Output Low-Dropout Regulator Optimized for Microprocessor Applications**

The LT1528 is a 3-amp low-dropout regulator with a quiescent current of 300 $\mu$ A. This device is optimized to handle the large output current transients associated with the current generation of microprocessors. This device has the fastest transient response of all currently available PNP regulators and is very tolerant of variations in capacitor ESR. Dropout voltage is 75mV at 10mA, rising to 200mV at 1A and 500mV at 3A. Quiescent current is well controlled in dropout mode; it does not increase significantly as the device enters its dropout region. The LT1528 can operate with output capacitors as small as 3 $\mu$ F, although larger capacitors will be needed to achieve the performance required in most microprocessor applications. Although the LT1528 is available with a fixed output voltage of 3.3V, the external sense pin allows the user to adjust the output to voltages greater than 3.3V with a simple resistive divider. This allows the device to be adjusted easily over a wide range of output voltages, including the 3.3V to 4.2V range required by a variety of microprocessors from Intel, IBM, and Cyrix.

The LT1528 has both reverse input and reverse output protection. The LT1528 includes a shutdown feature. Quiescent current drops to 150 $\mu$ A in shutdown mode. The LT1528 is available in a 5-lead TO-220 package.

**LT1529: 3-Amp PNP-Output, Low-Dropout Regulator Has Micropower Quiescent Current**

The LT1529 is a 3-amp low-dropout regulator with a quiescent current of only 30 $\mu$ A. Dropout voltage is 100mV at 10mA and rises to 500mV at 3A. Quiescent current is well controlled in dropout mode; it does not increase significantly as the device enters its dropout region. The device can operate with output capacitors as small as 3 $\mu$ F.

The LT1529 has both reverse-battery and reverse-output protection. Reverse output current is only 15 $\mu$ A, making this device ideal for backup power applications. The LT1529 includes a shutdown feature. Quiescent current drops to just 15 $\mu$ A in shutdown mode. The LT1529 is available in fixed output voltages of 3.3V and 5.0V. It is also available as an adjustable device with an output voltage range of 3.75V to 20V. The LT1529 is available in a 5-lead TO-220 package.

**The LTC1480: RS485 from 3.3V**

RS485 transceivers enter the 3.3V era with the introduction of the new LTC1480. Operating from a single 3.3V supply, the LTC1480 is fully compliant with all RS485 specifications. The LTC1480 features a maximum quiescent current of 500 $\mu$ A in driver-disable mode and 600 $\mu$ A in the driver-enable mode. It also provides a shutdown feature, which reduces the current consumption to below 1 $\mu$ A when the receiver and driver are disabled at the same time. Its driver uses a proprietary CMOS output stage that connects two Schottky diodes in series with the MOS output transistors. This allows the outputs to maintain high impedance when driven across the RS485 common-mode range (12V to -7V), or when the power is off. The driver's outputs also feature short-circuit protection and thermal shutdown.

The LTC1480 features half-duplex operation at up to 2.5Mbaud, with receiver and driver propagation delay of 200ns (max) and 80ns (max) respectively. The LTC1480 is offered in 8-pin DIP and SOIC packages, in both commercial and industrial temperature grades.

**LTC1487: Ultra-Low-Power 5V RS485 Transceiver with High Input Impedance**

The LTC1487 is an improved substitute for the LTC1483, designed with a high input impedance of 96k $\Omega$  (typical) to allow up to 256 transceivers to

share a single RS485 differential data bus or line. With multiple transceivers operating over the differential bus, the LTC1487 is fully compliant with all RS485 specifications. The LTC1487 features remarkably low current, the lowest ever in the industry. It has a maximum quiescent current of 120 $\mu$ A in receiver-active mode and 200 $\mu$ A in driver-active mode under no-load conditions. Significant power is saved by reducing quiescent current to below 1 $\mu$ A in the shutdown mode when both the receiver and the driver are disabled. Like the other members of LTC's RS485 transceiver family, the LTC1487 uses a unique fabrication process and design that includes Schottky diodes in series with the MOS output transistors, allowing the output to maintain high impedance when driven across the full RS485 common-mode range (12V to -7V) or when the power is off. The driver outputs also feature short-circuit protection and thermal shutdown.

The LTC1487 features half-duplex operation at up to 250kbaud, with receiver input propagation delay of less than 250ns. Its driver slew rate is deliberately limited to reduce EMI levels in the transmitted signal. The LTC1487 is available in 8-pin DIP and SOIC packages, in commercial temperature grades. **LT**

**For further information on the above or any of the other devices mentioned in this issue of *Linear Technology*, use the reader service card or call the LTC literature service number: 1-800-4-LINEAR. Ask for the pertinent data sheets and application notes.**

Burst Mode™ is a trademark of Linear Technology Corporation. **LT**, LTC and LT are registered trademarks used only to identify products of Linear Technology Corp. Other product names may be trademarks of the companies that manufacture the products.

Information furnished by Technology Corporation is believed to be accurate and reliable. However, Linear Technology makes no representation that the circuits described herein will not infringe on existing patent rights.

## DESIGN TOOLS

### Applications on Disk

#### NOISE DISK

This IBM-PC (or compatible) program allows the user to calculate circuit noise using LTC op amps, determine the best LTC op amp for a low noise application, display the noise data for LTC op amps, calculate resistor noise, and calculate noise using specs for any op amp. Available at no charge.

#### SPICE MACROMODEL DISK

This IBM-PC (or compatible) high density diskette contains the library of LTC op amp SPICE macromodels. The models can be used with any version of SPICE for general analog circuit simulations. The diskette also contains working circuit examples using the models, and a demonstration copy of PSPICE™ by MicroSim. Available at no charge.

## Technical Books

**1990 Linear Databook, Volume I** — This 1440 page collection of data sheets covers op amps, voltage regulators, references, comparators, filters, PWMs, data conversion and interface products (bipolar and CMOS), in both commercial and military grades. The catalog features well over 300 devices. \$10.00

**1992 Linear Databook Supplement** — This 1248 page supplement to the *1990 Linear Databook* is a collection of all products introduced since then. The catalog contains full data sheets for over 140 devices. The *1992 Linear Databook Supplement* is a companion to the *1990 Linear Databook*, which should not be discarded. \$10.00

**1994 Linear Databook, Volume III** — This 1826 page supplement to the *1990 Linear Databook* and *1992 Linear Databook Supplement* is a collection of all products introduced since 1992. A total of 152 product data sheets are included with updated selection guides. The *1994 Linear Databook Volume III* is a supplement to the 1990 and 1992 Databooks, which should not be discarded. \$10.00

**Linear Applications Handbook • Volume I** — 928 pages full of application ideas covered in depth by 40 Application Notes and 33 Design Notes. This catalog covers a broad range of "real world" linear circuitry. In addition to detailed, systems-oriented circuits, this handbook contains broad tutorial content together with liberal use of schematics and scope photography. A special feature in this edition includes a 22 page section on SPICE macromodels. \$20.00

**1993 Linear Applications Handbook • Volume II** — Continues the stream of "real world" linear circuitry initiated by the *1990 Handbook*. Similar in scope to the 1990 edition, the new book covers Application Notes 41 through 54 and Design Notes 33 through 69. Additionally, references and articles from non-LTC publications that we have found useful are also included. \$20.00

**Interface Product Handbook** — This 424 page handbook features LTC's complete line of line driver and receiver products for RS232, RS485, RS423, RS422, V.35 and AppleTalk® applications. Linear's particular expertise in this area involves low power consumption, high numbers of drivers and receivers in one package, mixed RS232 and RS485 devices, 10kV ESD protection of RS232 devices and surface mount packages. Available at no charge.

**SwitcherCAD Handbook** — This 144 page manual, including disk, guides the user through SwitcherCAD—a powerful PC software tool which aids in the design and optimization of switching regulators. The program can cut days off the design cycle by selecting topologies, calculating operating points and specifying component values and manufacturer's part numbers. \$20.00

**1995 Power Solutions Brochure, First Edition** — This 64 page collection of circuits contains real-life solutions for common power supply design problems. There are over 45 circuits, including descriptions, graphs and performance specifications. Topics covered include PCMCIA power management, microprocessor power supplies, portable equipment power supplies, micropower DC/DC, step-up and step-down switching regulators, off-line switching regulators, linear regulators and switched capacitor conversion. Available at no charge.

## World Headquarters

**Linear Technology Corporation**  
1630 McCarthy Boulevard  
Milpitas, CA 95035-7487  
Phone: (408) 432-1900  
FAX: (408) 434-0507

## U.S. Area Sales Offices

**CENTRAL REGION**  
**Linear Technology Corporation**  
Chesapeake Square  
229 Mitchell Court, Suite A-25  
Addison, IL 60101  
Phone: (708) 620-6910  
FAX: (708) 620-6977

**NORTHEAST REGION**  
**Linear Technology Corporation**  
3220 Tillman Drive, Suite 120  
Bensalem, PA 19020  
Phone: (215) 638-9667  
FAX: (215) 638-9764

**Linear Technology Corporation**  
266 Lowell St., Suite B-8  
Wilmington, MA 01887  
Phone: (508) 658-3881  
FAX: (508) 658-2701

**NORTHWEST REGION**  
**Linear Technology Corporation**  
782 Sycamore Dr.  
Milpitas, CA 95035  
Phone: (408) 428-2050  
FAX: (408) 432-6331

**SOUTHEAST REGION**  
**Linear Technology Corporation**  
17000 Dallas Parkway  
Suite 219  
Dallas, TX 75248  
Phone: (214) 733-3071  
FAX: (214) 380-5138

**SOUTHWEST REGION**  
**Linear Technology Corporation**  
22141 Ventura Blvd.  
Suite 206  
Woodland Hills, CA 91364  
Phone: (818) 703-0835  
FAX: (818) 703-0517

## International Sales Offices

**FRANCE**  
**Linear Technology S.A.R.L.**  
Immeuble "Le Quartz"  
58 Chemin de la Justice  
92290 Chatenay Malabry  
France  
Phone: 33-1-41079555  
FAX: 33-1-46314613

**GERMANY**  
**Linear Technolgy GmbH**  
Untere Hauptstr. 9  
D-85386 Eching  
Germany  
Phone: 49-89-3197410  
FAX: 49-89-3194821

**JAPAN**  
**Linear Technology KK**  
5F NAO Bldg.  
1-14 Shin-Ogawa-Cho, Shinjuku-Ku  
Tokyo, 162 Japan  
Phone: 81-3-3267-7891  
FAX: 81-3-3267-8010

**KOREA**  
**Linear Technology Korea Branch**  
Namsong Building, #505  
Itaewon-Dong 260-199  
Yongsan-Ku, Seoul  
Korea  
Phone: 82-2-792-1617  
FAX: 82-2-792-1619

**SINGAPORE**  
**Linear Technology Pte. Ltd.**  
507 Yishun Industrial Park A  
Singapore 2776  
Phone: 65-753-2692  
FAX: 65-541-4113

**TAIWAN**  
**Linear Technology Corporation**  
Rm. 602, No. 46, Sec. 2  
Chung Shan N. Rd.  
Taipei, Taiwan, R.O.C.  
Phone: 886-2-521-7575  
FAX: 886-2-562-2285

**UNITED KINGDOM**  
**Linear Technology (UK) Ltd.**  
The Coliseum, Riverside Way  
Camberley, Surrey GU15 3YL  
United Kingdom  
Phone: 44-276-677676  
FAX: 44-276-64851

## LINEAR TECHNOLOGY CORPORATION

1630 McCarthy Boulevard  
Milpitas, CA 95035-7487

(408) 432-1900

Literature Department 1-800-4-LINEAR

